

PERFORMANCE EVALUATION OF MASONRY

INFILL WALLS

PROJECT REPORT



Submitted by

TOM K ISAC

ROLL NO: M20CESC15

Department of Civil Engineering

T.K.M College of Engineering, Kollam-691005

A P J Abdul Kalam Technological University

2022

DECLARATION

I undersigned hereby declare that the project report “Performance Evaluation of Masonry Infill walls”, submitted for partial fulfilment of the requirements for the award of degree of Master of Technology of the APJ Abdul Kalam Technological University, Kerala is a bonafide work done by me under supervision of Prof. Bushra M.A, Assistant Professor, Department of Civil Engineering. This submission represents my ideas in my own words and where ideas or words of others have been included; I have adequately and accurately cited and referenced the original sources. I also declare that I have adhered to ethics of academic honesty and integrity and have not misrepresented or fabricated any data or idea or fact or source in my submission. I understand that any violation of the above will be a cause for disciplinary action by the institute and/or the University and can also evoke penal action from the sources which have thus not been properly cited or from whom proper permission has not been obtained. This report has not been previously formed the basis for the award of any degree, diploma or similar title of any other University.

Kollam

20/06/2022

TOM K ISAC

**Thangal Kunju Musaliar College of
Engineering,**

Kollam, Kerala

Department of Civil Engineering

CERTIFICATE

This is to certify that this project report entitled

**PERFORMANCE EVALUATION OF MASONRY
INFILL WALLS**

Submitted by

TOM K ISAC

Roll no: M20CESC15

*in the year 2022 in partial fulfilment of the requirement for the award of degree of
Master of Technology in Civil Engineering by*

the

A P J Abdul Kalam Technological University

Guide



Prof. Bushra M. A.

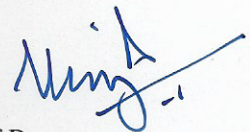
Assistant Professor,
Dept. of Civil Engg.,
TKMCE, Kollam.

Co-ordinator

Dr. Ramaswamy K. P.

Assistant Professor,
Dept. of Civil Engg.,
TKMCE, Kollam.

Head of Department



Dr. Sajeed R.

Professor,
Dept. of Civil Engg.,
TKMCE, Kollam.

ACKNOWLEDGEMENT

I would like to express my deep and sincere gratitude to Prof. Bushra M. A., Assistant Professor, Dept. of Civil Engineering, TKM College of Engineering for her valuable guidance, motivation, utmost care and kindness shown at every stage of my project preparation.

I would also like to express my grateful acknowledgement to Dr. Ramaswamy K. P., Assistant Professor, Dept. of Civil Engineering, TKM College of Engineering for providing me an opportunity to present this project.

I am greatly thankful to Dr. Sajeeb R., Professor and Head of the Department of Civil Engineering, for her kind support.

Finally, I wish to express my sincere thanks to my friends for their kind suggestions, encouragements and intangible support during the preparation and presentation of this project.

Above all, I thank the almighty God for the successful conduct of this project.

TOM K ISAC

ABSTRACT

Infill walls are very common structure present around us but their significance was always overlooked leading to the premature collapse of building during the laterals loads such as earthquake and wind loads. After many drastic failures of masonry buildings, civil engineers try to find the answer for the failure of these buildings. Later, studies show that the infill walls play an important role when the lateral loads are applied on to the structure.

Engineers also found that it is very difficult to conduct experimental studies by changing different parameters of the infill walls. So, researchers have been finding other simpler methods to analyse the infill walls to get the actual behaviour of the structure under lateral loading. This leads to the formulation of numerical modelling so that the behaviour can be easily analysed by simply changing the parameters as well as the material properties.

This thesis paper is set out to study the effect of lateral loading on an unconfined masonry, effect of confining frame, effect of lintel beams and effect of size of openings and their orientations using ANSYS software. Performance of each models were studied by comparing the load carrying capacity, initial lateral stiffness and energy dissipation capacity.

Keywords: Masonry infill walls, failure mechanism, numerical analysis, lateral loads, load carrying capacity, lateral stiffness, energy dissipation capacity, drift ratio.

CONTENTS

| | |
|--|------|
| ACKNOWLEDGEMENT | i |
| ABSTRACT | ii |
| LIST OF FIGURES | viii |
| LIST OF TABLES | x |
| CHAPTER 1: INTRODUCTION | 1 |
| 1.1. General | 1 |
| 1.2. Significance of work | 4 |
| 1.3. Objectives | 4 |
| 1.4. Scope | 5 |
| CHAPTER 2: LITERATURE REVIEW | 6 |
| 2.1 Influence of masonry infill walls on performance of building | 6 |
| 2.2. Influence of openings on performance of walls | 8 |
| 2.3. Influence of height of masonry walls on its performance | 10 |
| 2.4. Influence of boundary conditions on performance of walls | 10 |
| 2.5. Influence of lintel beams on performance of walls | 11 |
| 2.6. Influence of different brick bonds on performance of walls | 12 |
| 2.7. Summary of literature review | 12 |
| 2.8. Research gaps | 12 |
| CHAPTER 3: METHODOLOGY | 13 |
| 3.1. General | 13 |
| 3.2. Analysis procedure | 14 |

| | |
|------------------------------------|----|
| CHAPTER 4: VALIDATION | 15 |
| 4.1. Journal data | 15 |
| 4.2. Inputting material properties | 16 |
| 4.3. Meshing | 16 |
| 4.4. Boundary conditions | 17 |
| 4.5. Result and comparison | 17 |
| CHAPTER 5: GEOMETRIC MODELLING | 19 |
| 5.1 General | 19 |
| 5.2. Modelling | 19 |
| 5.2.1. SOLID186 | 19 |
| 5.2.2. CONTA174 and TARGE170 | 19 |
| 5.2.3. REINF264 | 19 |
| 5.3. Meshing | 20 |
| 5.3.1. General | 20 |
| 5.3.2. Processor details | 20 |
| 5.3.3. Mesh convergence | 20 |
| CHAPTER 6: ANALYSIS | 21 |
| 6.1. Material Properties | 21 |
| 6.1.1. Masonry | 21 |
| 6.1.2. Concrete | 21 |
| 6.1.3. Reinforcement steel | 21 |
| 6.2. Setup | 21 |
| 6.2.1. Unconfined infill walls | 21 |

| | |
|--|----|
| 6.2.1.1. General | 21 |
| 6.2.1.2. Samples | 22 |
| 6.2.1.3. Loading pattern and boundary conditions | 23 |
| 6.2.2. Masonry infill walls with confining frame | 23 |
| 6.2.2.1. General | 23 |
| 6.2.2.2. Samples | 23 |
| 6.2.2.3. Reinforcement details | 24 |
| 6.2.2.4. Loading pattern and boundary conditions | 25 |
| 6.2.3. Masonry infill walls with confining frame and lintel beam | 26 |
| 6.2.3.1. General | 26 |
| 6.2.3.2. Samples | 26 |
| 6.2.3.3. Reinforcement details | 27 |
| 6.2.3.4. Loading pattern and boundary conditions | 28 |
| 6.2.4. Masonry walls with openings | 29 |
| 6.2.4.1. General | 29 |
| 6.2.4.2. Samples | 29 |
| 6.2.4.3. Reinforcement details | 32 |
| 6.2.4.4. Loading pattern and boundary conditions | 32 |
| CHAPTER 7: RESULTS AND DISCUSSIONS | 33 |
| 7.1. Performance evaluation of unconfined infill walls | 33 |
| 7.1.1. Load carrying capacity | 33 |
| 7.1.1.1. Influence of length of wall | 33 |
| 7.1.1.2. Influence of height of wall | 34 |

| | |
|--|----|
| 7.1.1.3. Influence of thickness of wall | 35 |
| 7.1.2. Lateral stiffness | 36 |
| 7.1.3. Energy dissipation | 38 |
| 7.2. Performance evaluation of masonry infill walls with confining frame | 39 |
| 7.2.1 Failure mechanism | 39 |
| 7.2.2. Load carrying capacity | 40 |
| 7.2.3. Lateral stiffness | 41 |
| 7.2.4. Energy dissipation | 42 |
| 7.3. Performance evaluation of masonry infill walls with lintel beams | 43 |
| 7.3.1. Load carrying capacity | 43 |
| 7.3.2. Lateral stiffness | 44 |
| 7.3.3. Energy dissipation | 44 |
| 7.4. Performance evaluation of masonry infill walls with openings | 46 |
| 7.4.1. Effect of size of openings | 46 |
| 7.4.1.1. Load carrying capacity | 46 |
| 7.4.1.2. Lateral stiffness | 47 |
| 7.4.1.3. Energy dissipation | 47 |
| 7.4.2. Effect of placement of openings | 48 |
| 7.4.1.1. Load carrying capacity | 48 |
| 7.4.1.2. Lateral stiffness | 49 |
| 7.4.1.3. Energy dissipation | 50 |
| CHAPTER 8: CONCLUSIONS | 51 |
| 8.1. General | 51 |

| | |
|----------------------|----|
| 8.2. Major findings | 51 |
| 8.3. Future scope | 52 |
| REFERENCES | 53 |
| LIST OF PUBLICATIONS | 57 |

LIST OF FIGURES

| FIG NO. | TITLE | PAGE NO |
|--------------------|--|--------------------|
| 1.1 | Masonry infill walls | 1 |
| 1.2 | Behaviour of masonry infill walls | 2 |
| 1.3 | Detailed micro-modelling | 3 |
| 1.4 | Simplified micro-modelling | 3 |
| 1.5 | Macro-modelling | 4 |
| 3.1 | Research methodology | 13 |
| 4.1 | Pushover analysis | 15 |
| 4.2 | Input parameters | 16 |
| 4.3 | Meshing details | 16 |
| 4.4 | Boundary condition and loading pattern | 17 |
| 4.5 | Variation of base shear | 17 |
| 4.6 | Parity curve for top displacement | 18 |
| 4.7 | Parity curve for base shear | 18 |
| 5.1 | Force deformation curve | 20 |
| 6.1 | Stress-strain curve of masonry | 21 |
| 6.2 | Loading and boundary conditions | 23 |
| 6.3 | Samples | 24 |
| 6.4 | Reinforcement detailing | 25 |
| 6.5 | Loading and boundary conditions | 25 |
| 6.6 | Samples | 26 |
| 6.7 | Reinforcement detailing | 27 |
| 6.8 | Loading and boundary conditions | 28 |
| 6.9 | Samples | 30 |

| | | |
|------|---|----|
| 6.10 | Samples | 30 |
| 7.1 | Load-drift ratio curve | 33 |
| 7.2 | Load-drift ratio curve | 34 |
| 7.3 | Load-drift ratio curve | 35 |
| 7.4 | Variation of Load with respect to changes in wall dimensions | 36 |
| 7.5 | Lateral stiffness-drift ratio curve | 37 |
| 7.6 | Variation of lateral stiffness with respect to changes in wall dimensions | 37 |
| 7.7 | Hysteresis loop | 38 |
| 7.8 | Cumulative energy dissipation curve | 39 |
| 7.9 | Failure mechanism | 40 |
| 7.10 | Load-drift ratio curve | 40 |
| 7.11 | Lateral stiffness-drift ratio curve | 41 |
| 7.12 | Hysteresis loop | 42 |
| 7.13 | Cumulative energy dissipation curve | 42 |
| 7.14 | Load-drift ratio curve | 43 |
| 7.15 | Lateral stiffness-drift ratio curve | 44 |
| 7.16 | Hysteresis loop | 45 |
| 7.17 | Cumulative energy dissipation curve | 45 |
| 7.18 | Load-drift ratio curve | 46 |
| 7.19 | Lateral stiffness-drift ratio curve | 47 |
| 7.20 | Cumulative energy dissipation curve | 48 |
| 7.21 | Load-drift ratio curve | 49 |
| 7.22 | Lateral stiffness-drift ratio curve | 49 |
| 7.23 | Cumulative energy dissipation curve | 50 |

LIST OF TABLES

| TABLE NO. | TITLE | PAGE NO |
|----------------------|------------------------------------|--------------------|
| 6.1 | Details of unconfined infill walls | 22 |
| 6.2 | Details of samples with openings | 31 |

CHAPTER 1

INTRODUCTION

1.1. GENERAL

Infill walls are common elements present in buildings. Infill walls are mainly provided in between the moment resisting frame after the construction of the structural skeleton as shown in Fig.1.1

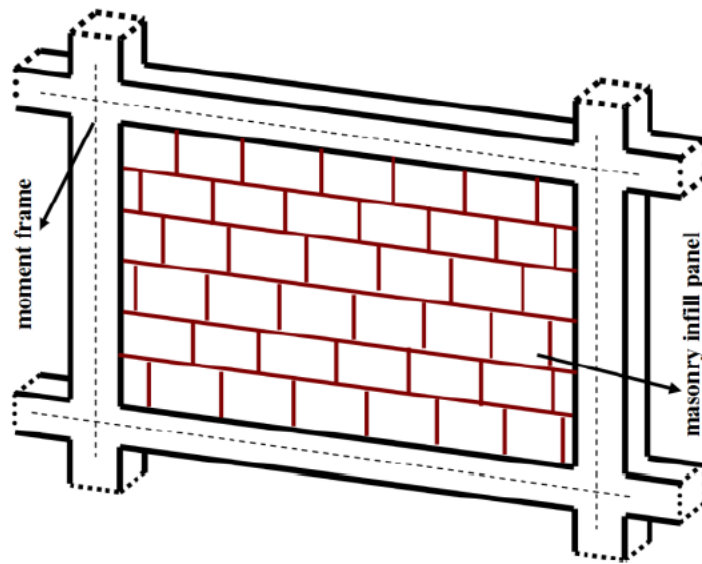


Fig.1.1 Masonry infill walls (Dilmac et al., 2018)

The main function of infill walls is to provide privacy and to have better space utilization. Commonly clay bricks, hollow bricks and autoclaved aerated concrete (AAC) blocks, etc has been used as infill materials. The supporting frame may be of reinforced concrete or steel structure.

Earlier days, the role of infill walls was neglected, but after many earthquakes they had found that infill wall plays an important role in determining the failure pattern of the structure. So, researchers started studying the behaviour of infill walls subjected to lateral loads.

Mainly there are three types of failure that can occur in a masonry infilled framed structure such as

- Diagonal cracking- On the action of lateral loads compressive force is induced in one diagonal and tension in other diagonal resulting in appearing of cracks in diagonal manner.
- Horizontal slip- In this, due to the action of loading, failure can occur in horizontal plane along the weaker mortar joints.
- Corner crushing - This is the result of the development of compression and tension in both diagonals. Due to this, the masonry wall at the opposite corners crushes onto the surrounding frame.

Pallares et al., 2021 studied the typical failure behaviour of an infill walled frame. We can see from Fig.1.2 that at the top left end and bottom right end of the frame, the frame just bears onto the infill walls which results in crushing or compression of the masonry units at that corner. At the same time, on the top right end we can see that the contact between the infill wall and the frame is lost. This is mainly due to the development of tension on one diagonal and compression on other diagonal.

Also, we can see that some 45° cracks passing through the body of infill wall. This is due to the development of tensile force in the diagonals. Due to lateral load, there occurs a tension as well as a compression force in diagonals. Since the bricks are generally weak in tensile force, cracking can occur in this diagonal area.

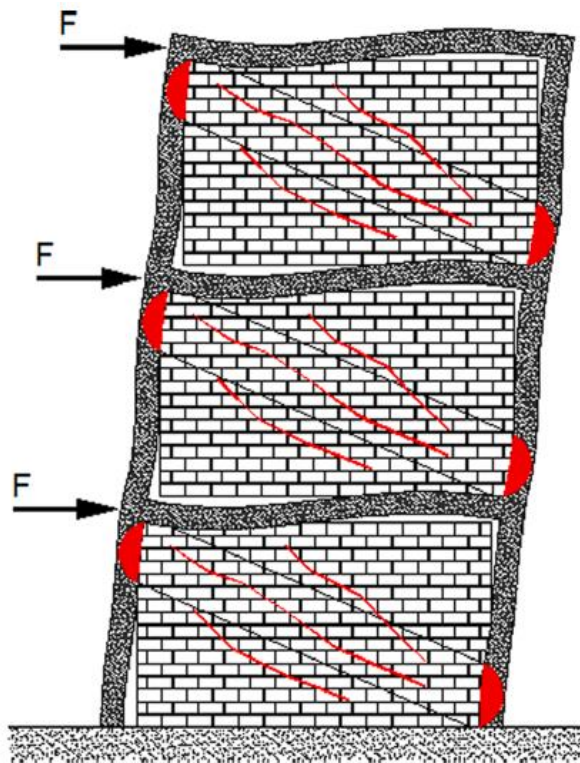


Fig.1.2 Behaviour of masonry infill walls (Pallares et al., 2021)

Since there are different changing parameters involved in the infill walls, experimental studies were not feasible. This resulted in creating different numerical models to study the behaviour of infill walls. Numerical analysis can be done in different methods like equivalent diagonal strut method and continuum method.

In equivalent static method, we model the infill wall into a diagonal compression element. It is an approximate method of analysis. But in continuum approach, we make use of a finite element package to model the whole structure. This is the most accurate method. In finite element method itself we can do it in 3 different ways:

- Detailed micro-modelling

In this method all the elements are modelled using special elements and after analysis we will get the complete failure mechanisms of the structure

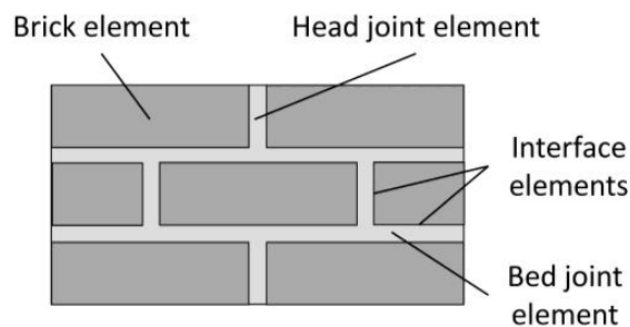


Fig.1.3 Detailed micro-modelling (Campbell and Duran, 2015)

- Simplified micro-modelling

In this, the bricks are modelled as special elements available in any finite element software package. But the mortar interface is modelled as a contact element. Since the mortar joint between the bricks are modelled as contact elements, Poisson's ratio of the mortar is neglected in this approach.

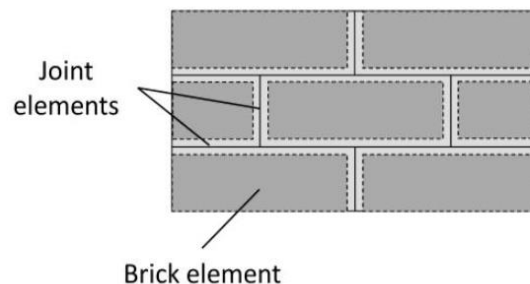


Fig.1.4 Simplified micro-modelling (Campbell and Duran, 2015)

- Macro-modelling

In this method, we are converting the whole structure into a single unit. Here we will be defining the failure criteria for the material and the analysis result will be an approximate one. This is the simplest type of analysis.

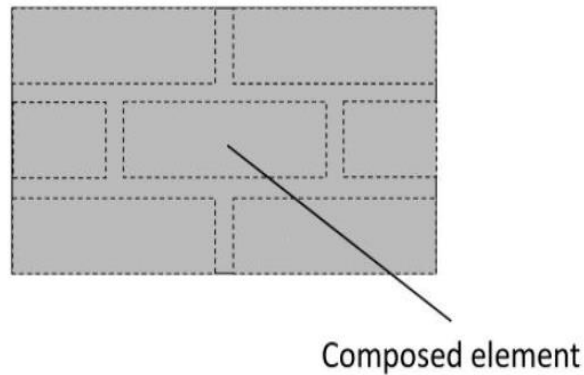


Fig.1.5 Macro-modelling (Campbell and Duran, 2015)

Nowadays infill walls are also considered as an important member in the design phase itself so that we can eliminate any premature collapse of building and prevent loss of life during lateral loadings.

In our study we are interested in macro-modelling of the structure.

1.2. SIGNIFICANCE OF WORK

Earlier days, researchers considered infill walls as a non-structural element or a secondary element during design phase. They assume the loads coming on to the building will be resisted by the primary elements like beams and columns. But after many disastrous earthquakes they have found out that masonry infill wall plays a crucial role in determining the load carrying capacity of the building. This leads to many experimental and numerical studies considering different parameters in infill walls.

1.3. OBJECTIVES

Research objectives developed are as follows:

- To study the performance of unconfined infill walls by changing the length, height and thickness of wall.
- To study the effect of confinement in infill walls.
- To study the change in failure behaviour of the infilled frame with lintel beams.

- To study the effect of combination of door and window opening in infill walls in determining the performance of the structure during lateral loading.

1.4. SCOPE

- Only numerical analysis has been done.
- Macro-modelling is done
- Modelling of a singular wall has been done rather than taking the whole structure.
- Out of plane loading as well as out of plane behaviour of the structure were not studied.

CHAPTER 2

LITERATURE REVIEW

2.1. INFLUENCE OF MASONRY INFILL WALLS ON PERFORMANCE OF BUILDING

Mehrabi et al., (1996) had conducted experimental evaluation of masonry infilled RC frames. They had designed two specimens: one designed for moderate wind loads and other for strong earthquake motions. Also, they had used solid and hollow concrete masonry panels for their study. They had found that the infill walls significantly affect the performance of the framed structures. In specimens with weak frames and strong infill panels, brittle failure was observed.

Keyvani & Farzadi (2011) studied the influence of infill walls on seismic performance of the frame using ANSYS. Results shows that ductility of the frame is dependent on the height up to which the masonry is provided and they had found out that only in frame with infill walls up to the total height resulted in improvement in ductility. They had also found that infilled frame improves the lateral stiffness of the building compared to that of a bare frame.

Tamboli & Karadi (2012) studied the influence of infill walls during the earthquake loads using ETABS. Infilled frame was modelled as an equivalent compression strut. Different parameters like base shear, storey drift, time period of oscillation of the building were investigated and found out that the infilled frame decreases the storey drift and time period of oscillation of the building compared to the bare frame. Also, the most practical case of open first storey was investigated and found out that the storey drift of the first storey was much higher than that of the bare frame as well as the fully infilled frame.

Campbell & Duran (2015) studied the possibility of developing a numerical model for accurately interpreting the in-plane behaviour of the masonry walls under seismic loads in ANSYS. They had taken a simplified micro modelling approach in which the mortar joints were assumed as link elements. Results showed the comparisons of the push over analysis of the infill walls with that of the values already available.

Thomas & Kuriakose (2016) studied the behaviour of the unreinforced masonry using ANSYS. They had done a macro-modelling in which they had reduced the masonry as

a single homogeneous unit and the parameters were defined to make the unit behave nonlinearly when load is applied. They had found out that with the increase in length as well as the width of the infill wall, the load carrying capacity of the structure is also increased.

Kumbasaroglu et al., (2017) studied the influence of bond slips between the infill wall and frame. For this they had done experiments on a bare frame, infilled frame with and without anchor bars. Results shows that the infilled frame with the anchor bars resulted in higher lateral strength, energy dissipation than the others. They had also found out that the displacement due to bond slippage of reinforcement bars resulted in nonlinear behaviour of frame.

Nasiri & Liu (2017) had developed a 3D finite element model for analysing the behaviour of masonry infilled concrete frames. A simplified micro modelling approach was followed in their study. They had found that the numerical analysis can be used to successfully replicate the actual behaviour of the masonry wall.

Dilmac et al., (2018) studied the seismic performance of existing buildings with and without infill wall using SAP 2000. They had considered the non-linear behaviour of concrete and the infill walls were designed as nonlinear strut elements, so that accurate results can be obtained. The results shows that if the infill walls are distributed uniformly, they can improve the performance of the building against the lateral loads. They also found out that the presence of infill walls resulted in increase in lateral stiffness, strength and energy dissipation compared to a bare frame.

Jalaeefar & Zargar (2018) had studied the effect of infill walls with special moment resisting frames subject to seismic loads. They had found that inclusion of infill walls had resulted in increasing the lateral stiffness and ultimate strength but had resulted in decrease in ductility of the structure.

Khan et al., (2019) studied the influence of brick masonry walls on seismic response of RC structures. They had modelled 3 models: one a bare frame second one a framed structure with infill walls and third one a framed infill structure with an open ground storey. They had found that the open ground storey and structure with infill walls shows increase in base shear than that of bare frame. Also, the relative displacement of the frame with masonry wall is lesser than that of bare frame.

Okasha et al., (2020) studied the effects of autoclaved aerated concrete (AAC) blocks as infill wall material on the seismic performance of the building using ETABS and ANSYS. A model with anchor bars protruding from the frame to the masonry was also studied. Results shows that infill wall made of AAC blocks not only reduces the dead weight of the building but also outperforms clay blocks in terms of in-plane stiffness and the reduction in storey drift. They have also found that the model with anchor bars resulted in reduction in displacement of the structure and increase in the failure load.

Furtado et al., (2021) studied the effect of infill walls on the floor response spectra of an 8-storey RC building. They had found out that the peak infill acceleration was always higher than peak floor acceleration. They had also found out that bare frame models showed higher displacement demands whereas the models with infill walls showed higher acceleration demands.

Pallares et al., (2021) studied the effect of masonry in determining the seismic behaviour of the building. Based on the experimental data a more simplified macro model was developed for the future study. Results shows that the masonry infill walls increase the stiffness of the building as a whole and also helps in reduction of fundamental period of oscillation.

2.2. INFLUENCE OF OPENINGS ON SEISMIC PERFORMANCE OF WALLS

Koutromanos et al., (2011) studied the possibility of numerical modelling of masonry infill walls due earthquake loads. Different failure behaviour was assigned to mortar, brick as well as the reinforced concrete member to get the actual behaviour of the infilled frame as a whole when an earthquake is acting upon it. They had found out that the inelastic behaviour of the infilled frame was not really sensitive to the lateral loading.

Uva et al., (2012) studied the seismic response of infilled frame as well as the bare frame using push over analysis. Infilled walls were designed as equivalent diagonal struts. Effect of openings in infill walls in determining the behaviour of failure was also studied. Increase in storey drift of about 50 % was seen by the introduction of openings in infill walls and it influences the performance of the building during earthquake loads.

Motwani et al., (2015) studied the influence of openings in the infill walls using ANSYS. They had found out that by providing masonry walls, the behaviour of the building to the lateral loading changes from flexure failure to axial action. Also, they had noticed that if the openings are placed on the main diagonal, it can seriously decrease the loads carrying capacity of the frame and thereby resulting in premature failure of the building.

Borsaikia & Dutta (2021) studied the participation of masonry in the linear and nonlinear behaviour of concrete along with the additions of openings in infill walls. The results show that with the increase in the size of the openings, the storey stiffness had been reduced considerably and also, they had observed that for openings of size more than 45 %, the contribution of the infill walls on the stiffness of the buildings is marginable.

Furtado et al., (2021) had conducted experimental and numerical assessment of confined infill walls with openings and textile reinforced mortar. They had found that openings had reduced the strength by 40% and the energy dissipation capacity by 18%. They had also concluded that textile reinforced mortar had resulted in increasing the initial stiffness by 31%, and the energy dissipation by 38%.

Pachappoyil & Agarwal (2021) had studied the Energy Dissipating Hysteretic (EDH) infill walls with openings. In this system, it consists of slotted concrete blocks and the connection is done by energy dissipating links (EDLs). EDLs are rubber tires sandwiched between steel plates. They had found out that the EDH infilled frame shows an improvement over the conventional masonry infill wall. Even after providing opening, Performance of EDH is better than that of conventional one. They also found out that the reduction in strength in EDH models with openings are proportional to the number of EDLs removed.

Rahem et al., (2021) had studied the effect of masonry wall with openings on nonlinear response of steel frames. They had found out that with the addition of infill walls the stiffness and the overall strength of the frame is improved. And they also found out that the size of opening has a significant effect on determining the overall strength and stiffness of the structure. They had also found that vertical openings lead to larger displacement than the horizontal ones.

2.3. INFLUENCE OF HEIGHT OF MASONRY WALLS ON ITS PERFORMANCE

Guevara & Garcia (2005) studied influence of height of the masonry infill wall on the failure behaviour of the structure during the earthquake loads. They had found that the provision of masonry infill walls up to the total height resulted in increasing the lateral stiffness of the structure and there by resulting in a more predictable failure pattern of the building frame whereas by providing the infill wall only up to a certain height resulted in developing higher force on the column region which is not laterally supported and thereby resulting in short column effect.

Baniahmadi et al., (2022) had studied the cyclic response of reinforced concrete frames partially filled with relatively weak infill panels. They had found out that partially infilled columns exhibited more cracks at the mid height compared that that of bare frames. They had also found that ultimate strength of partially filled frames are around 50% more than that of bare frames.

2.4. INFLUENCE OF BOUNDARY CONDITIONS ON PERFORMANCE OF WALLS

Marinkovic & Butenweg (2019) studied various decoupling systems in infill walls for seismic protection. In this new system called Innovative Decoupled infilled system (INODIS), they had introduced a combination of U-shaped elastomer with glued joints in between the joints of masonry wall and the frame. They had compared the performance of this new system with traditional decoupling mechanisms and had found that the new system resulted in delaying the in-plane activation of infill wall, reduces the stresses coming onto the specimen, and also allowed larger inter-storey drift of more than 3%.

Bikce et al., (2021) studied the performance of non-interacting infill walls due to the in-plane loading. Study had been conducted experimentally and thereafter a numerical model was also analysed using ABAQUS. They have found out that the non-interacting infill walls resulted in a failure behaviour which is almost similar to that of a bare frame but it had less lateral load capacity that that of an infilled frame.

Dhir et al., (2021) had conducted a numerical modelling of reinforced concrete frames with infill walls and rubber joints using ABAQUS software. They had placed horizontal

joints at three levels and vertical rubber joints at the both sides of the masonry wall abutting the surrounding frame. They had found that the introduction of the rubber joints resulted in reduction in damages in the masonry wall.

Pudjisuryadi et al., (2021) studied the in-plane as well as the out-plane behaviour of the infill wall along with the introduction of friction base support on infill walls. For simplicity, infill walls were modelled as equivalent diagonal struts. Results shows that for buildings with friction base support, the inter-storey drifts were much lesser that that of fixed base infill walls.

2.5. INFLUENCE OF LINTEL BEAMS ON PERFORMANCE OF WALLS

Stravroulaki & Liarakos (2012) studied seismic analysis of masonry infill wall with concrete lintel beams by changing the friction coefficients between lintel beam and the masonry infill wall. They had found out that the introduction of lintel beams helped in reducing the plastic strain when the lintel beam is in contact with masonry infill wall. They had also found that sliding effect of the lintel beam and masonry infill wall reduces the energy dissipation capacity of the structure.

Park et al., (2013) studied whether lintel beams had any significant role in resisting the lateral loading. Results from their studies show that lintel beam resulted in improving the energy dissipation of the structure. They had also found out that the presence of lintel beams had no effect in elastic region as it only come into effect in the plastic region.

Deb et al., (2021) studied the behaviour of the infill walls with lintel beams numerically. A nonlinear dynamic analysis has been done to study the behaviour of the building. They had found that by providing tie beams or lintel beams in infill walls, it converts the masonry infill wall into a confined one, which in turn increases the collapse time of the structure.

Shendkar et al., (2021) studied the possibility of unreinforced masonry walls and semi-interlocked masonry infill wall along with lintel beams. They had found out that average base shear developed for a frame with semi-interlocked bricks with lintel beams is much more than that of unreinforced masonry infill wall with lintel beams. Also, they have found out that the model with lintel beams show lower value for response reduction factor compared to the value specified in IS 1893(Part I):2016

2.6. INFLUENCE OF DIFFERENT BRICK BONDS ON PERFORMANCE OF WALLS

Naciri et al., (2022) studied the influence of brick shape and bond pattern in the seismic performance of building. In their study they had also proposed the use of new brick shape as well as new bond (PLUS bond). They had found that the newly proposed bond improves ductility and energy dissipation and of the structure under cyclic loading.

2.7. SUMMARY OF LITERATURE REVIEW

Based on the literature survey we had understood that there are different parameters that can affect the performance of infill walls subjected to lateral loads. Based on the previous studies we had found that the length, height and thickness of the wall can affect the behaviour of the masonry walls. Also, by providing confining frame and lintel beams, the strength and capacity is improved drastically. They had also found out that by changing the boundary condition the failure pattern of the masonry wall can be altered. Also, by providing openings the load carrying capacity was reduced.

2.8. RESEARCH GAPS

Gaps identified from the literature survey are as follows:

- Effect of height to thickness ratio of infill walls were not studied.
- Studied related to orientation of combination of openings were very less.
- Studies incorporating the effect of lintel beams on infill walls were very less.
- Studies related to the different bond patterns in brick masonry were very less.
- Studies related to different boundary conditions were very less.

CHAPTER 3

METHODOLOGY

3.1. GENERAL

The behaviour of masonry walls is complex when an earthquake is acting upon it, so doing many iterative experiments to generalise the findings is a much more complex procedure. So, a numerical modelling is better suited in this situation.

The project is done on a finite element package called ANSYS. Here we will be inputting the material parameters and we will be modelling the infill wall along with the surrounding frame and various parameters like opening size, their placement in wall, combination of opening, height and thickness of wall, boundary condition of wall, frame characteristics and provision of lintel beams are changed and the comparison between these results are to be done.

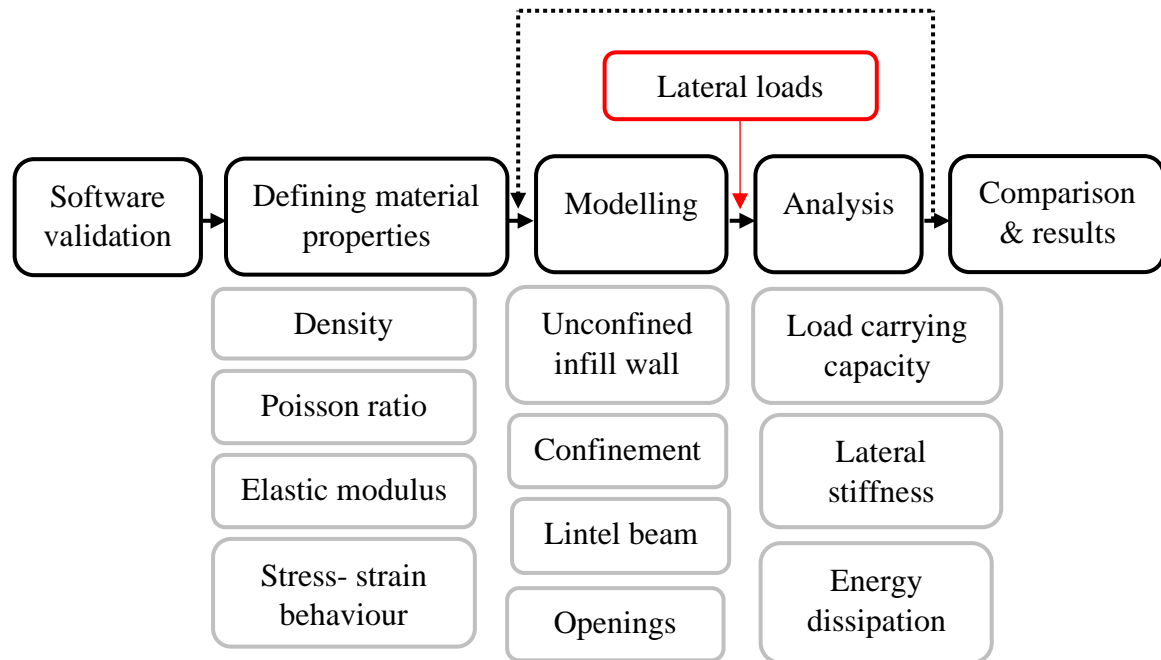


Fig.3.1 Research methodology

3.2. ANALYSIS PROCEDURE

Step 1: Defining material properties

First of all, we will be inputting all the properties of all the materials to be used in the model. We will be defining the compressive strength of the concrete to be used, the stress-strain behaviour of concrete, steel and masonry, density of these materials, Elastic modulus and Poisson ratio, etc.

Step 2: Modelling

In our study we will be using macro-modelling technique i.e., the brick masonry wall is modelled as a single unit.

First of all, we are interested in finding the behaviour of the unconfined masonry wall. For that we will be changing the length, height and thickness of the wall.

Next, we will be adding a confinement frame and lintel beams to study their influence on the performance. Here the interface between concrete frame and masonry wall is defined as frictional surface.

Lastly, we will be adding openings in the masonry wall and we will be changing their size and their placement or orientation to the study the effect on performance.

Step 3: Analysis

After the modelling of the structure, we will be inputting the monotonic lateral loads and cyclic loads and we will be evaluating the structure by plotting the load-drift ratio curve, lateral stiffness curve and energy dissipation curve also.

Step 4: Comparison

After analysing the structure, we will be generalising the parameters and will be comparing the results of each model to get a clear picture. From the results we will be arriving at the most possible scenario which can improve the seismic performance of the structure as a whole.

CHAPTER 4

VALIDATION

4.1. JOURNAL DATA

Masonry unit is modelled using SOLID65 model available in ANSYS software. The whole masonry was assumed to be acting as a single unit. A masonry tower of 6m (length) x 3m (width) x 0.4m (height) was modelled using ANSYS software. The failure pattern of the masonry unit is assumed to be Drucker-Prager model. A simple pushover analysis was done on the model to get the plot between maximum base shear and displacement. For push over analysis, a uniformly distributed load of q kN/m is applied on the side of the building. Size of the mesh was 0.3m. The maximum base shear developed was found out to be 174 kN and failure has occurred at maximum displacement of 0.17m

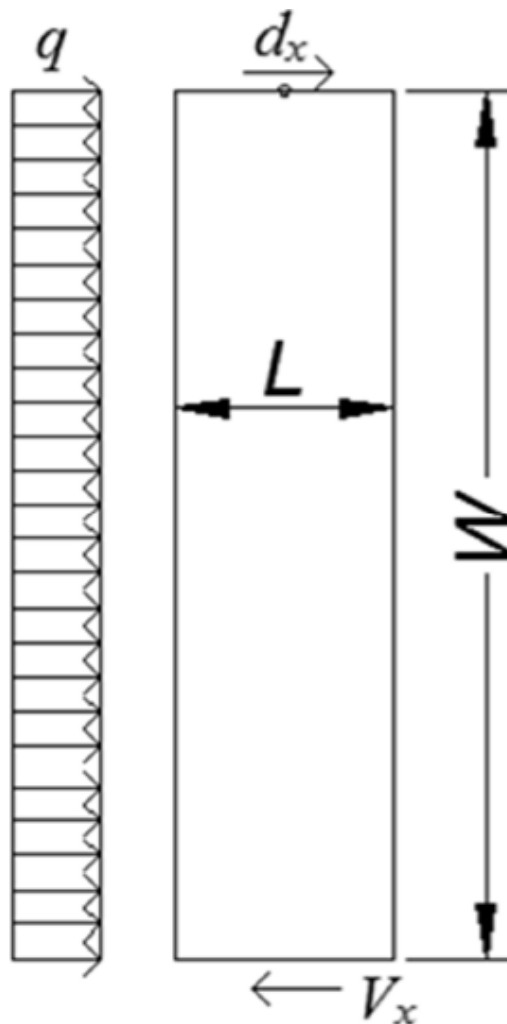


Fig.4.1 Pushover analysis (Thomas & Kuriakose, 2016)

4.2. INPUTTING MATERIAL PROPERTIES

First of all, the material properties of the masonry units are inputted to the ANSYS software. Also, the Drucker-Prager failure criteria was also inputted

| Properties of Outline Row 3: 0 | | | | |
|--------------------------------|--|-------------------|--------|---|
| | A | B | C | D E |
| 1 | Property | Value | Unit | <input checked="" type="checkbox"/> <input checked="" type="checkbox"/> |
| 2 | <input checked="" type="checkbox"/> Material Field Variables | Table | | <input type="checkbox"/> <input type="checkbox"/> |
| 3 | <input checked="" type="checkbox"/> Isotropic Elasticity | | | <input type="checkbox"/> <input type="checkbox"/> |
| 4 | Derive from | Young's Modulu... | | <input type="checkbox"/> <input type="checkbox"/> |
| 5 | Young's Modulus | 1.5E+09 | Pa | <input type="checkbox"/> <input type="checkbox"/> |
| 6 | Poisson's Ratio | 0.25 | | <input type="checkbox"/> <input type="checkbox"/> |
| 7 | Bulk Modulus | 1E+09 | Pa | <input type="checkbox"/> <input type="checkbox"/> |
| 8 | Shear Modulus | 6E+08 | Pa | <input type="checkbox"/> <input type="checkbox"/> |
| 9 | <input checked="" type="checkbox"/> Drucker-Prager | | | <input type="checkbox"/> <input type="checkbox"/> |
| 10 | <input checked="" type="checkbox"/> Drucker-Prager Base | | | <input type="checkbox"/> <input type="checkbox"/> |
| 11 | Uniaxial Compressive Strength | 5 | MPa | <input type="checkbox"/> <input type="checkbox"/> |
| 12 | Uniaxial Tensile Strength | 0.24 | MPa | <input type="checkbox"/> <input type="checkbox"/> |
| 13 | Biaxial Compressive Strength | 6 | MPa | <input type="checkbox"/> <input type="checkbox"/> |
| 14 | <input checked="" type="checkbox"/> Failure Plane Data Set 1 | | | <input type="checkbox"/> <input type="checkbox"/> |
| 15 | <input checked="" type="checkbox"/> Failure Plane | | | <input type="checkbox"/> <input type="checkbox"/> |
| 16 | Inner Friction Angle | 38 | degree | <input type="checkbox"/> <input type="checkbox"/> |
| 17 | Initial Cohesion | 1.2E+05 | Pa | <input type="checkbox"/> <input type="checkbox"/> |
| 18 | Dilatancy Angle | 15 | degree | <input type="checkbox"/> <input type="checkbox"/> |

Fig.4.2 Input parameters

4.3. MESHING

A masonry tower of 6m x 3m x 0.4m was modelled using ANSYS. Meshing was done with size of 0.3m. The masonry unit was modelled using SOLID186 element.

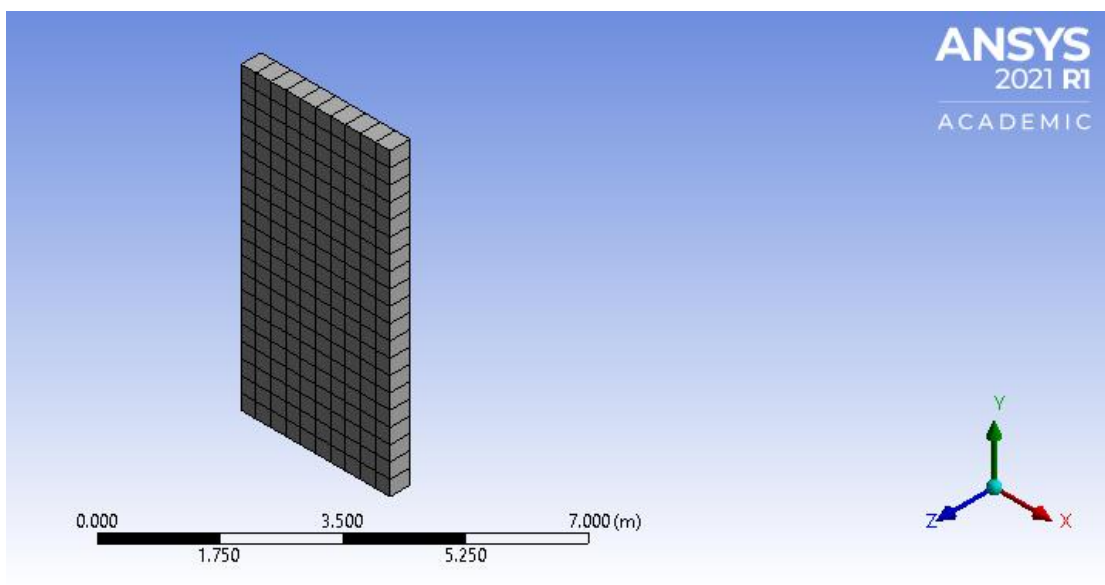


Fig.4.3 Meshing details

4.4. BOUNDARY CONDITIONS

Base of the masonry tower is fixed and load is applied on one of the sides as pressure.

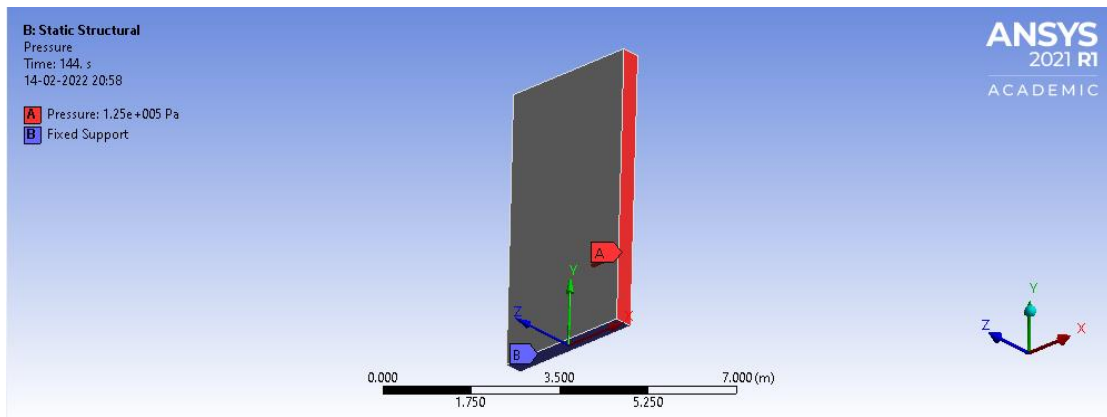


Fig.4.4 Boundary conditions and loading diagram

4.5. RESULT AND COMPARISON

After push over analysis, a graph between maximum base shear developed and displacement is plotted. After analysis, we have found out that the maximum base shear developed was 171 kN and failure has occurred at maximum displacement of 0.165m. The variation in maximum base shear developed was about 2 % and of maximum displacement 3%

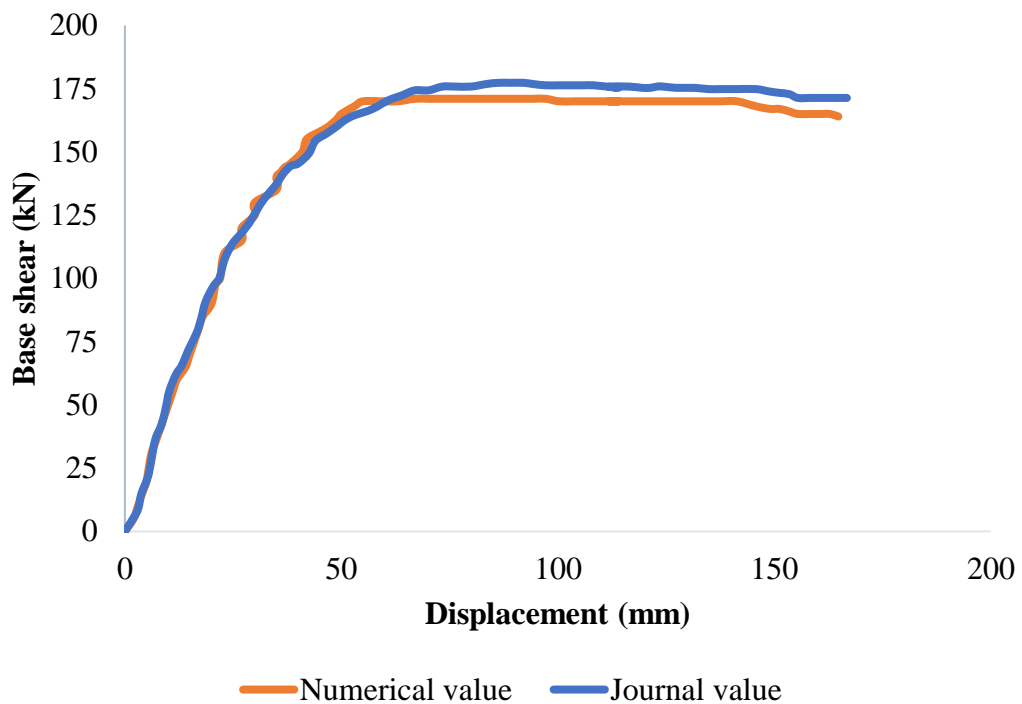


Fig.4.5 Variation of base shear

To get the actual variation of the obtained value with the journal data we had plotted a parity curve for displacement and base shear as shown in Fig.4.6 and Fig.4.7 respectively

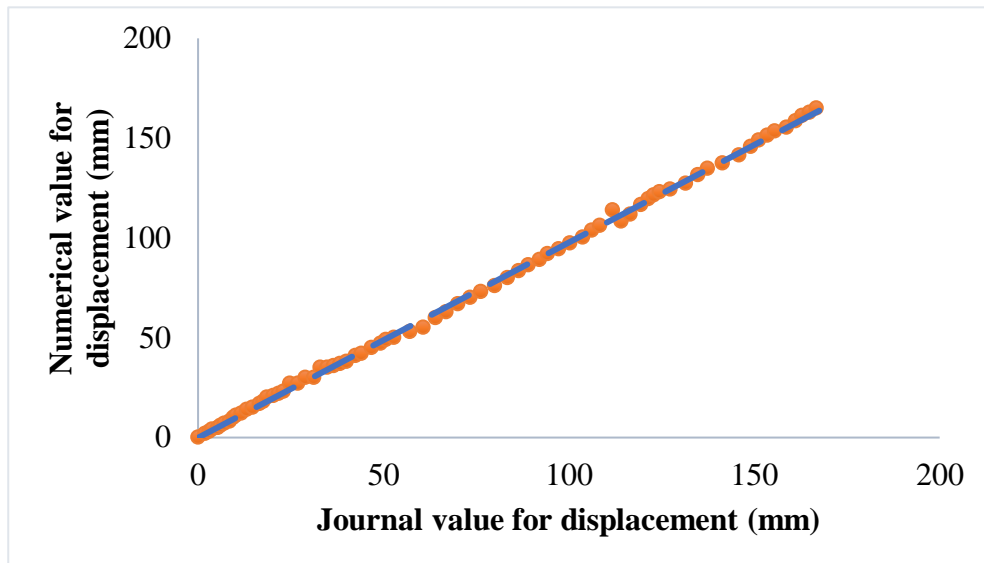


Fig.4.6 Parity curve for top displacement

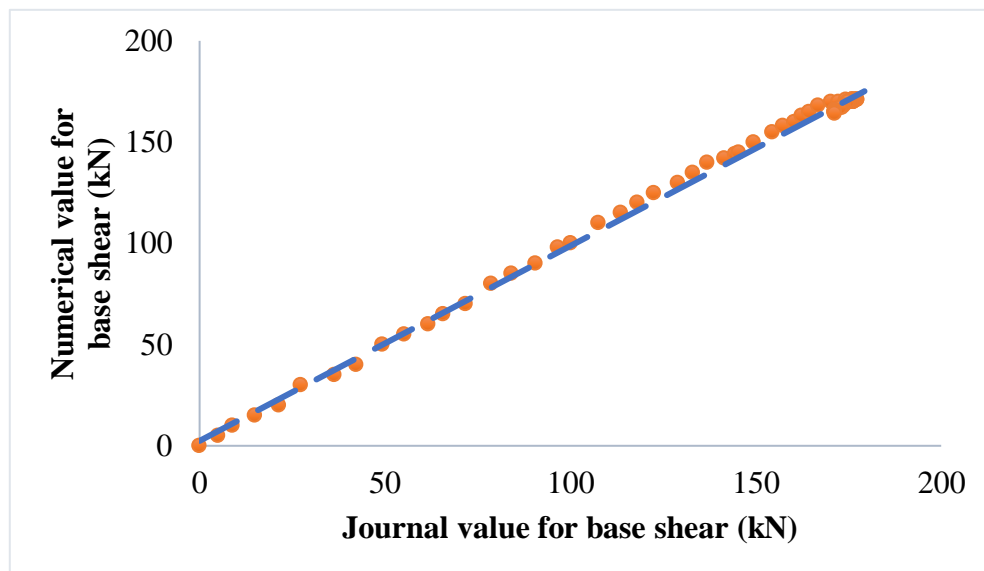


Fig.4.7 Parity curve for base shear

From the above graph it is clear that there is only a small deviation in the obtained value with the of the journal value. So, validation of the software is done.

CHAPTER 5

GEOMETRIC MODELLING

5.1. GENERAL

Masonry wall was modelled as a single homogenous unit rather than singular brick. In this, the combination of brick element and the mortar is taking as a single unit. By doing this we are neglecting the sliding failure between the brick units.

Concrete used for the confining frame is of compressive strength 40 MPa and the steel used for the rebar is of yield strength 250 MPa. The surface between the concrete the masonry wall is defined as frictional surface with frictional coefficient of 0.7.

5.2. MODELLING

Brick element and concrete had been modelled using SOLID186 element. Reinforcing bar has been modelled using REINF264 element. Contact surface has been modelled as CONTA174 and TARGE170 element

5.2.1. SOLID186

Solid 186 element is a 20 noded solid element used in ANSYS software. The element is defined by 20 nodes having three degrees of freedom per node i.e., translations in x, y, z directions. It is capable in simulating the deformations of incompressible elastoplastic materials

5.2.2. CONTA174 and TARGE170

CONTA174 is used to represent sliding contact between the surfaces and for pair-based target surfaces we use TARGE170.

5.2.3. REINF264

These are reinforcing element used to model the reinforcing steel. The degree of freedom and the number of nodes depends upon the base element used in the analysis.

5.3. MESHING

5.3.1. General

For analysis of complex shapes or models we use finite element analysis. One of the basic principles of the finite element analysis is discretisation i.e., dividing the complex geometry into smaller elements. So, the size of the mesh is very much important in determining the accuracy of result we get. The selection of the mesh is depended upon the processor capacity and the complexity of the model.

5.3.2. Processor details

Processor: 12th Gen Intel i5-12400, 2500 MHz, 6 Core(s), 12 Logical Processors

RAM: 16 GB

5.3.3. Mesh convergence

For studying the mesh convergence, we had taken an unconfined masonry wall with 1.8m length, 3.0m height and 0.1m thickness. The mesh size is changed from 50mm to 200mm and the plot between the load and deformation is shown in Fig.5.1

When we move from 50mm mesh to 200 mm mesh the overall change in maximum force attained is showing only about 2 % variation. So, we can conclude that change in mesh is not influencing the output so we had finalised in using 150 mm mesh in the analysis.

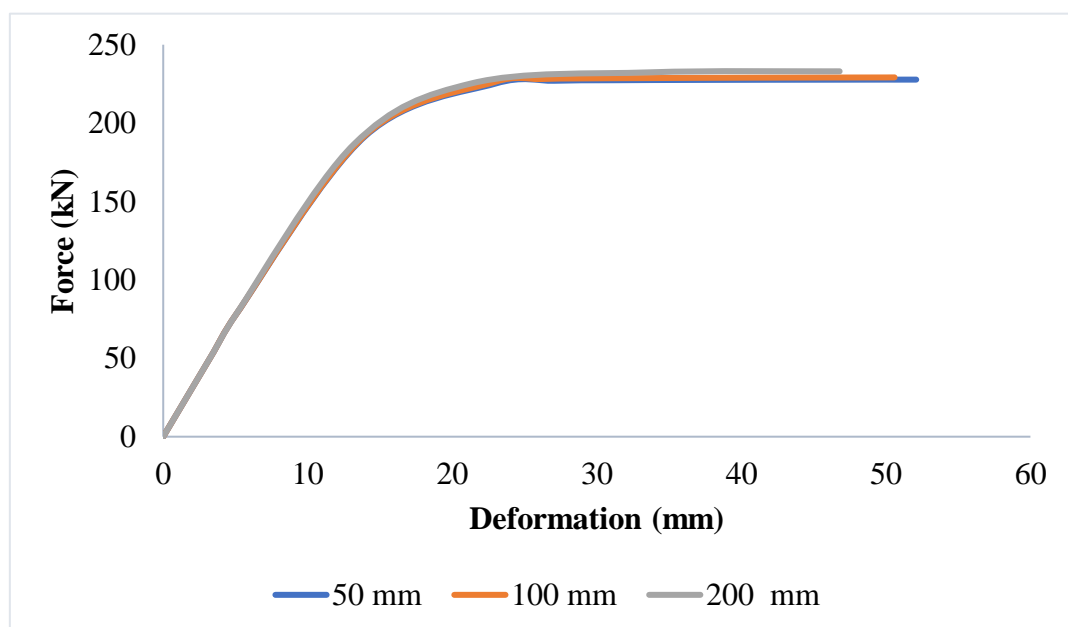


Fig.5.1 Force-deformation curve

CHAPTER 6

ANALYSIS

6.1. MATERIAL PROPERTIES

6.1.1. Masonry

For obtaining the properties of brick masonry we had collected the stress-strain relationship of brick masonry as shown in Fig.6.1.

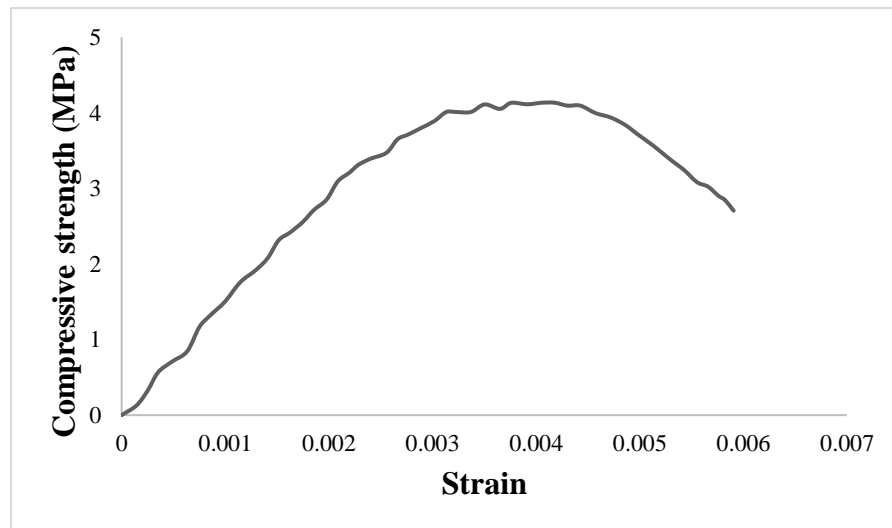


Fig.6.1 Stress-strain curve of masonry (Kaushik et al. 2007)

6.1.2. Concrete

Properties of concrete were taken similar to that defined in nonlinear general materials. The concrete defined in the software is of compressive strength 40MPa

6.1.3. Reinforcement steel

Properties of reinforcement steel were taken similar to that defined in nonlinear general materials. The steel defined in the software is of yield strength 250MPa

6.2. SETUP

6.2.1. Unconfined infill walls

6.2.1.1 General

In this setup, we had modelled the masonry wall as unconfined one i.e., we were not restraining the displacement. This resulted in unrestrained deformation in the direction of loading.

6.2.1.2. Samples

For studying the behaviour of the unconfined masonry structure, we were changing different parameters like length, thickness and height of the infill wall. In the case of length of wall, we had taken 1.8m, 2.5m and 3.0m for this study. In most buildings the masonry wall will in the range from 1.2m to 3.6m, so that is why we had taken the above-mentioned value. For thickness of wall, we had taken 0.1m and 0.2m thickness to simulate the half brick wall and one brick wall, which is commonly used. For height of the wall, we had taken 2.1m and 3.0m. In most of the residential buildings, the storey height is 3.0m and for some architectural purposes, some may be having the wall up to lintel beam (about 2.1m). Considering all these combinations, we had 12 models. Details of the models is displayed in the table below.

Table 6.1 Details of unconfined infill walls

| Sample No. | Length (m) | Height (m) | Thickness (m) | Designation |
|------------|------------|------------|---------------|-------------|
| 1 | 1.80 | 3.00 | 0.10 | 1.8*3*.1 |
| 2 | 1.80 | 3.00 | 0.20 | 1.8*3*.2 |
| 3 | 1.80 | 2.10 | 0.10 | 1.8*2.1*.1 |
| 4 | 1.80 | 2.10 | 0.20 | 1.8*2.1*.2 |
| 5 | 2.50 | 3.00 | 0.10 | 2.5*3*.1 |
| 6 | 2.50 | 3.00 | 0.20 | 2.5*3*.2 |
| 7 | 2.50 | 2.10 | 0.10 | 2.5*2.1*.1 |
| 8 | 2.50 | 2.10 | 0.20 | 2.5*2.1*.2 |
| 9 | 3.00 | 3.00 | 0.10 | 3*3*.1 |
| 10 | 3.00 | 3.00 | 0.20 | 3*3*.2 |
| 11 | 3.00 | 2.10 | 0.10 | 3*2.1*.1 |
| 12 | 3.00 | 2.10 | 0.20 | 3*2.1*.2 |

6.2.1.3. Loading pattern and boundary conditions

For analysis, we had fixed the bottom face of the masonry wall as shown in Fig.6.2 and we had inputted the acceleration due to gravity so that the self-weight will have an effect on the behaviour of the wall.

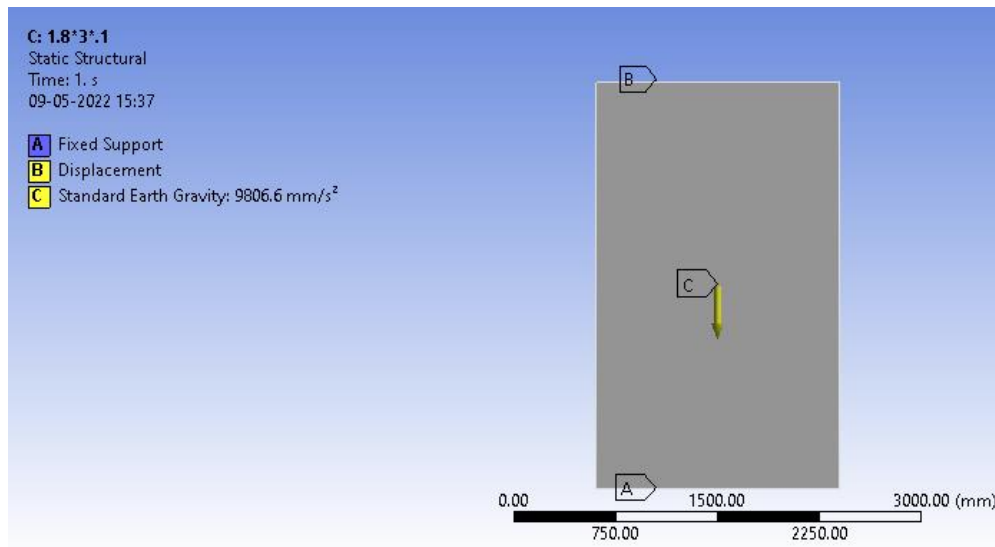


Fig.6.2 Loading and boundary conditions

Loadings on the models were given on the top face. The loading was done as displacement controlled one i.e., we applying a specified displacement on the top face instead of force. By using the ANSYS software we were able to find the force which was required to make that top displacement possible.

6.2.2. Masonry infill walls with confining frame

6.2.1.1 General

In this setup, we had modelled the masonry wall as confined one i.e., the lateral movement of the masonry wall was restricted by the presence of the confining frame.

6.2.2.2. Samples

For analysis purpose we had selected the model which is showing worst performance during the analysis of unconfined models. So, if we can show an improvement in the performance in that model, we can say that confining frame definitely improves the structure as a whole.

So, the model selected for this study was a masonry wall with 1.80m length, 3.0m height and 0.10m thick. For comparison purposes we had selected an unconfined and confined models of the same sample as shown in Fig.6.3.

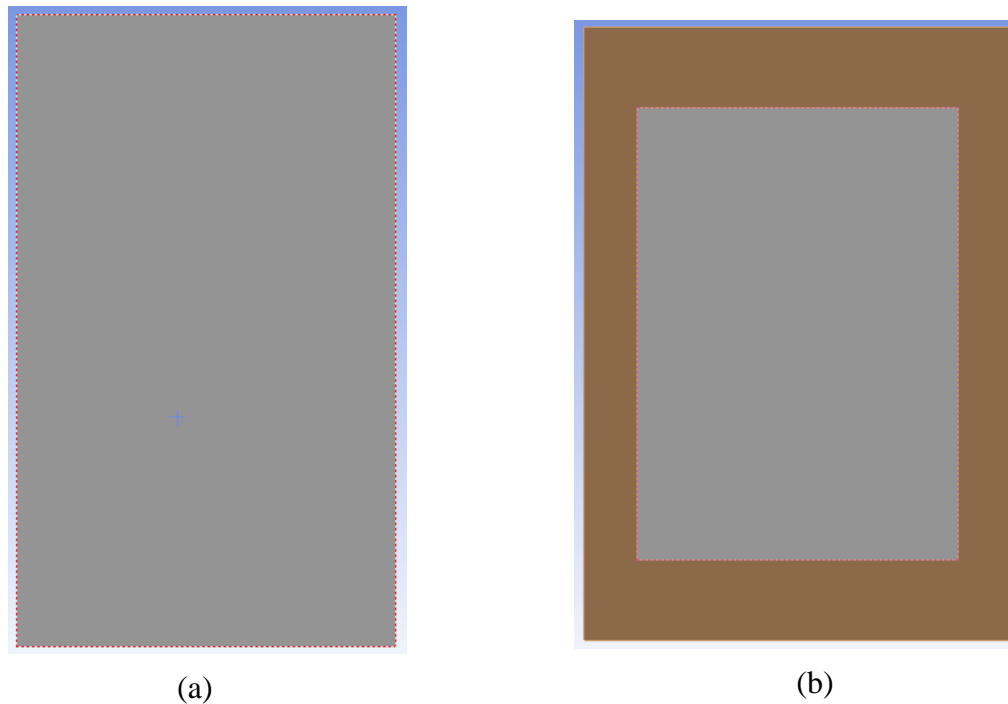


Fig.6.3 Samples (a) unconfined (b) with confinement frame

6.2.2.3. Reinforcement details

Reinforcement detailing of the confining frame is done in full compliance with IS 13920:2016.

Column details

- Column section – 300mm x 300mm
- Longitudinal reinforcement – 16mm Ø
- Stirrups – 8mm Ø @ 150mm spacing at centre and 100mm spacing near ends
- The area of steel provided is 0.89 % is well between the limits set by the IS codes [0.8 % (min) < 0.89 % < 6% (max)]

Beam details

- Beam section – 300mm x 450mm
- Longitudinal reinforcement – 20mm Ø at bottom and 12mm Ø at top face
- Stirrups – 8mm Ø @ 80mm centre to centre

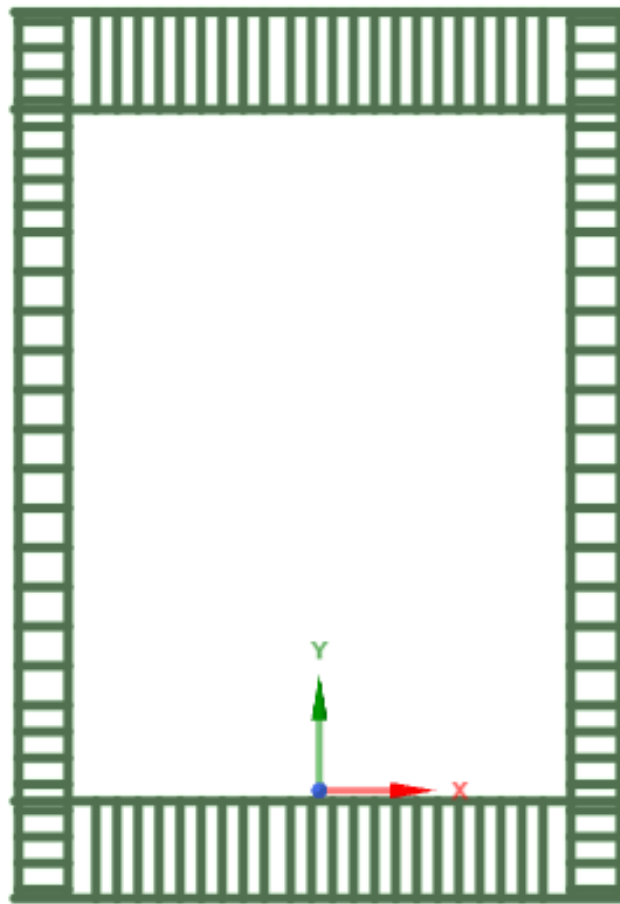


Fig.6.4 Reinforcement detailing

6.2.2.4. Loading pattern and boundary conditions

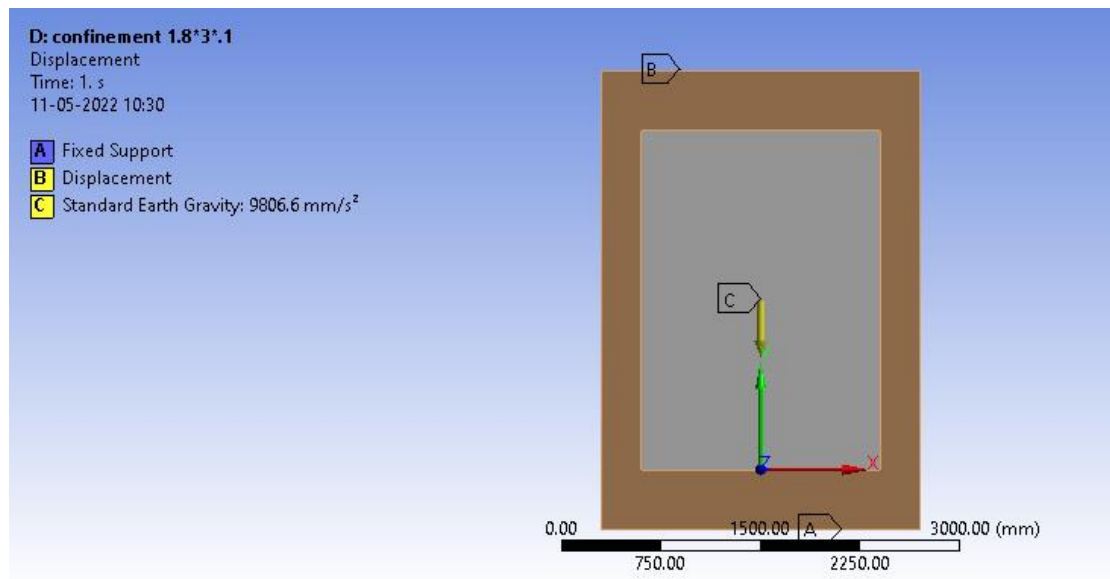


Fig.6.5 Loading and boundary conditions

Here also we had fixed the bottom face of the masonry wall as shown in Fig.6.5 and we had inputted the acceleration due to gravity so that the self-weight will have an effect on the behaviour of the wall. All the contact surfaces (interface between the concrete frame and the masonry wall) were modelled as frictional surface with frictional coefficient of 0.70.

Loading was given on the top face. We had applied monotonic loading for analysing the lateral load carrying capacity and lateral stiffness. But for computing the energy dissipation we had applied cyclic loading at the top face.

6.2.3. Masonry infill walls with confining frame and lintel beams

6.2.3.1 General

In this setup, we had modelled the masonry wall with confining frame with the addition of lintel beam. This created a confined effect to the masonry wall below the lintel level.

During analysis we were only interested in the failure of the masonry wall below the lintel level because the wall above the lintel level is stiff enough which could result in unreliable output.

6.2.3.2. Samples

The model selected for this study was a masonry wall with 1.80m length, 2.1m height and 0.10m thick. For comparison purposes we had selected a masonry wall with confining frame and a masonry wall with confining frame and lintel as shown in Fig.6.6

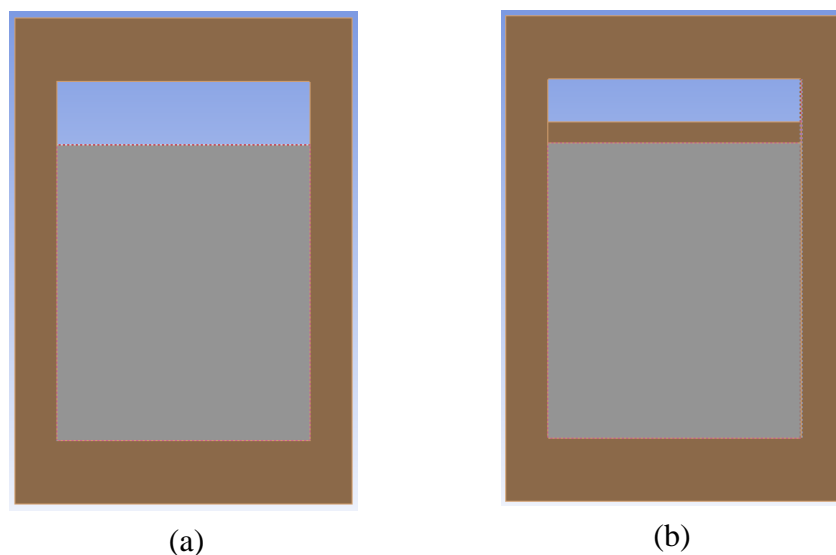


Fig.6.6 Samples (a) without lintel beam (b) with lintel beam

6.2.3.3. Reinforcement details

Here also reinforcement detailing of the confining frame is done in full compliance with IS 13920:2016.

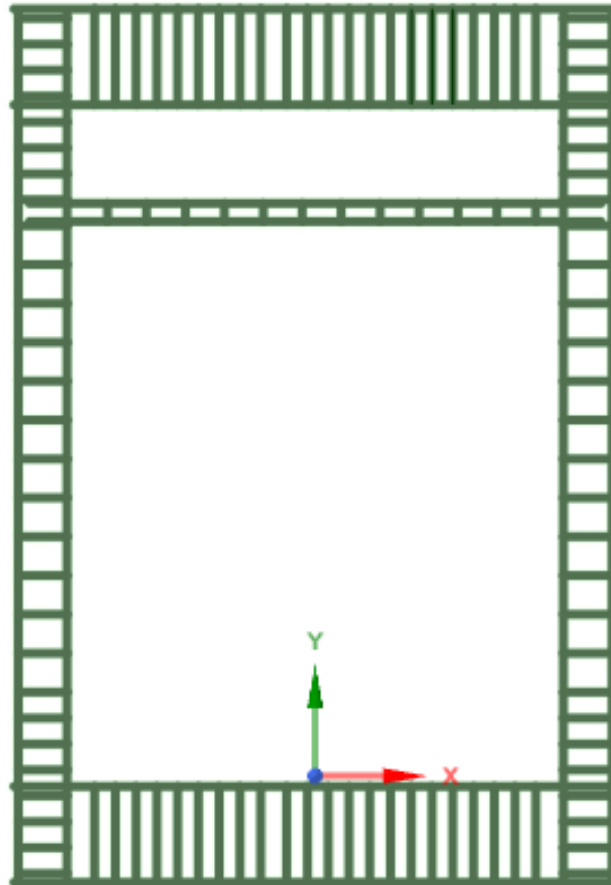


Fig.6.7 Reinforcement detailing

Column details

- Column section – 300mm x 300mm
- Longitudinal reinforcement – 16mm \emptyset
- Stirrups – 8mm \emptyset @ 150mm spacing at centre and 100mm spacing near ends
- The area of steel provided is 0.89 % is well between the limits set by the IS codes [0.8 % (min) < 0.89 % < 6% (max)]

Beam details

- Beam section – 300mm x 450mm
- Longitudinal reinforcement – 20mm \emptyset at bottom and 12mm \emptyset at top face
- Stirrups – 8mm \emptyset @ 80mm centre to centre

Lintel beam details

- Beam section – 100mm x 150mm
- Longitudinal reinforcement – 10mm \varnothing at bottom top face
- Stirrups – 8mm \varnothing @ 150mm centre to centre

6.2.3.4. Loading pattern and boundary conditions

Here also we had fixed the bottom face of the masonry wall as shown in Fig.6.8 and we had inputted the acceleration due to gravity so that the self-weight will have an effect on the behaviour of the wall. All the contact surfaces (interface between the concrete frame and the masonry wall) were modelled as frictional surface with frictional coefficient of 0.70. Loading was given on the top face. We had applied monotonic loading for analysing the lateral load carrying capacity and lateral stiffness. But for computing the energy dissipation we had applied cyclic loading at the top face.

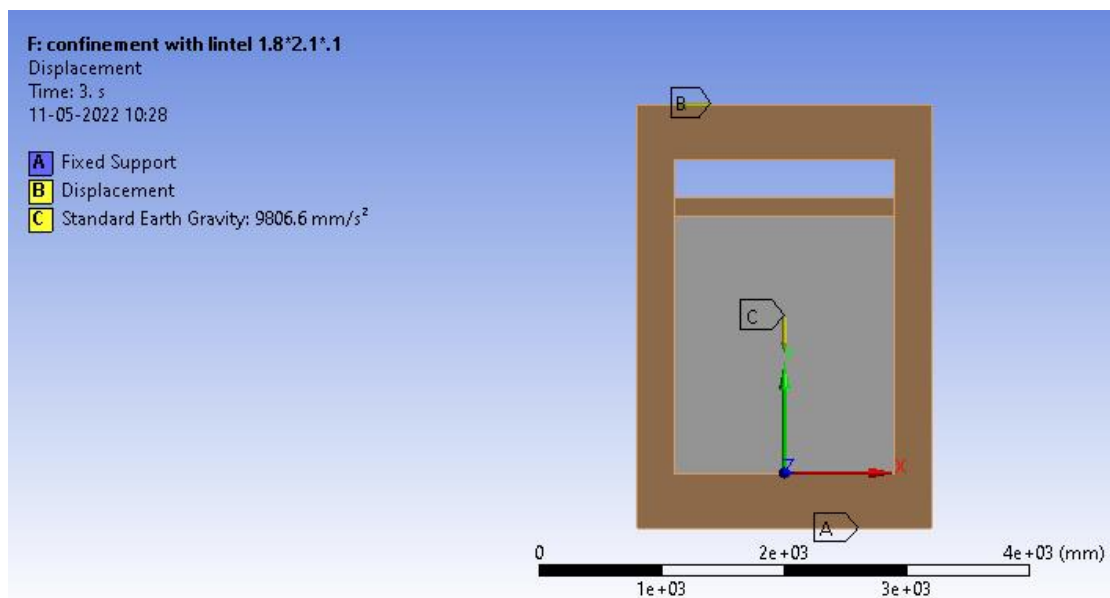


Fig.6.8 Loading and boundary conditions

6.2.4. Masonry infill walls with openings

6.2.4.1 General

In this setup, we had modelled the masonry wall with confining frame with the addition of lintel beam along with openings of varying size and different orientations to simulate the behaviour of the masonry also close to the real time conditions.

Here also we were only interested in the failure of the masonry wall below the lintel level because the wall above the lintel level is stiff enough can result in unreliable results. Here we are studying two aspects of opening first we will be studying the effect of size of opening and secondly, we will be studying the effect of placement of opening keeping the size of the opening as constant.

6.2.4.2. Samples

The model selected for this study was a masonry wall with 3.0m length, 3.0m height and 0.2m thickness.

For studying the effect of openings, we had used the door openings as 0.90m and 1.20m. In normal residential buildings the width of the door openings was 0.90m and for front door we would go for 1.20m.

In the case of window openings, we had used openings with width of 0.5m, 1.0m, 1.5m corresponding to one panelled, two-panelled and three-panelled windows. Also, we had changed the height of windows as 1.2m, 1.5m, and 1.8m corresponding to windows in the kitchen, normal window and French windows respectively.

Other parameter we had introduced is the placement of the openings i.e., whether the openings were placed eccentrically or centrally. Based on all these parameters we had 28 models. Details of the models is shown in Table 6.2.

For studying the influence of size of the opening, we had selected 49 and 83% opening size keeping the placement of openings as constant. In 49% opening size, we had incorporated 0.9m wide door placed eccentrically towards left end and a window of width 1.0m and 1.20m height and for 83 % opening size, a 1.2m wide door placed eccentrically towards left end and a window of width 1.5m width and 1.80m height as shown in Fig.6.9.

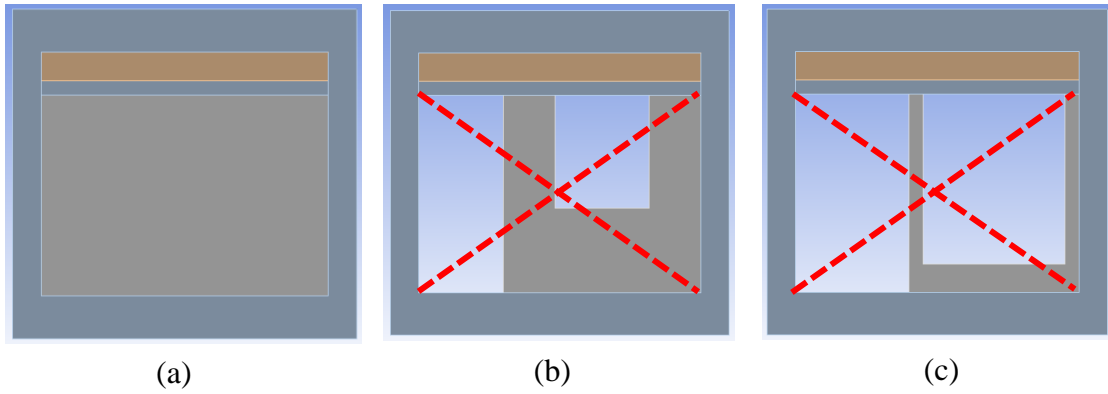


Fig.6.9 Samples (a) no opening (b) 49% opening (c) 83% opening

For studying the influence of placement of the opening, we had selected 59% opening size as constant and the placement of openings were changed as shown in Fig. 6.10. In Fig.6.10(b) 0.9*2.1 door is placed eccentrically towards left side and 1*1.2 window was placed eccentrically placed towards right side and in Fig.6.10(c) 1.2*2.1 door is placed eccentrically towards left side and 1.5*1.8 window was placed at the centre of the right side.

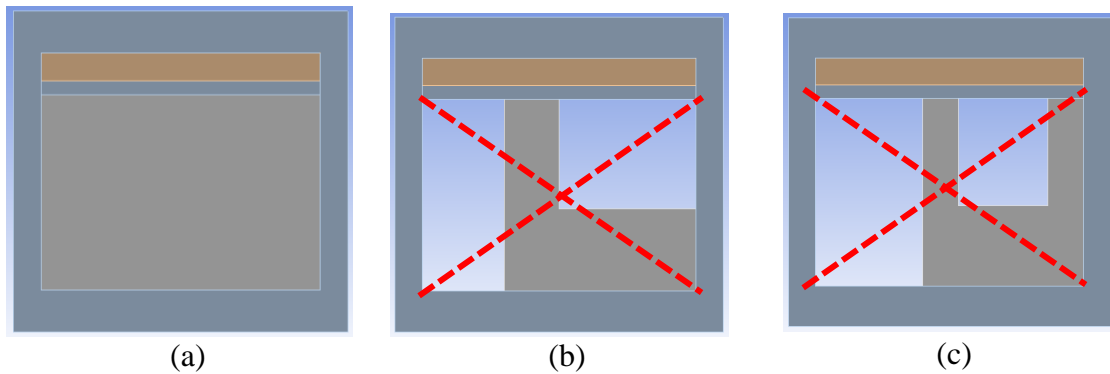


Fig.6.10 Samples (a) no opening (b) eccentrically placed window (c) centrally placed window

Table 6.2 Details of samples with openings

| Sl No. | Width of door (m) | Orientation | Window specification | | Orientation | Area of openings (%) |
|--------|-------------------|-----------------------|----------------------|------------------------|------------------------|----------------------|
| | | | Width (m) | Height (m) | | |
| 1 | 0.90m | Centre | 0.50 | 1.20 | Centre | 49 |
| 2 | | | 0.50 | 1.20 | Eccentrically to Right | |
| 3 | | Eccentrically to Left | 1.00 | 1.20 | Centre | |
| 4 | | | 1.00 | 1.20 | Eccentrically to Right | |
| 5 | | Centre | 0.50 | 1.50 | Centre | 54 |
| 6 | | | 0.50 | 1.50 | Eccentrically to Right | |
| 7 | | Eccentrically to Left | 1.00 | 1.50 | Centre | |
| 8 | | | 1.00 | 1.50 | Eccentrically to Right | |
| 9 | | | 1.50 | 1.20 | Centre | 59 |
| 10 | | | 1.50 | 1.20 | Eccentrically to Right | |
| 11 | | | 1.50 | 1.50 | Centre | 66 |
| 12 | | | 1.50 | 1.50 | Eccentrically to Right | |
| 13 | | 1.50 | 1.80 | Centre | 73 | |
| 14 | | | 1.80 | Eccentrically to Right | | |
| 15 | 1.20m | Centre | 0.50 | 1.20 | Centre | 59 |
| 16 | | | 0.50 | 1.20 | Eccentrically to Right | |
| 17 | | Eccentrically to Left | 1.00 | 1.20 | Centre | |
| 18 | | | 1.00 | 1.20 | Eccentrically to Right | |
| 19 | | Centre | 0.50 | 1.50 | Centre | 64 |
| 20 | | | 0.50 | 1.50 | Eccentrically to Right | |
| 21 | | Eccentrically to Left | 1.00 | 1.50 | Centre | |
| 22 | | | 1.00 | 1.50 | Eccentrically to Right | |
| 23 | | | 1.50 | 1.20 | Centre | 69 |
| 24 | | | 1.50 | 1.20 | Eccentrically to Right | |
| 25 | | | 1.50 | 1.50 | Centre | 76 |
| 26 | | | 1.50 | 1.50 | Eccentrically to Right | |
| 27 | | 1.50 | 1.80 | Centre | 83 | |
| 28 | | | 1.80 | Eccentrically to Right | | |

6.2.4.3. Reinforcement details

Section of beam, column and lintel beam and the reinforcement details are similar to that given in Fig.6.7

6.2.4.4. Loading pattern and boundary conditions

Here also we were interested in displacement-controlled loading. The loading is done on the top face and the bottom face is modelled as fixed support and the interface between the frame and the masonry wall is modelled as frictional surface with frictional coefficient of 0.7. which is similar to that in Fig.6.8

CHAPTER 7

RESULTS AND DISCUSSIONS

7.1. PERFORMANCE EVALUATION OF UNCONFINED INFILL WALLS

7.1.1. Load carrying capacity

7.1.1.1. Influence of length of wall

- To study the influence of the length of the infill wall, we have kept the other dimensions (thickness and height of the wall) as constant value as 0.1 and 3.0m respectively and only length of the wall is varied.

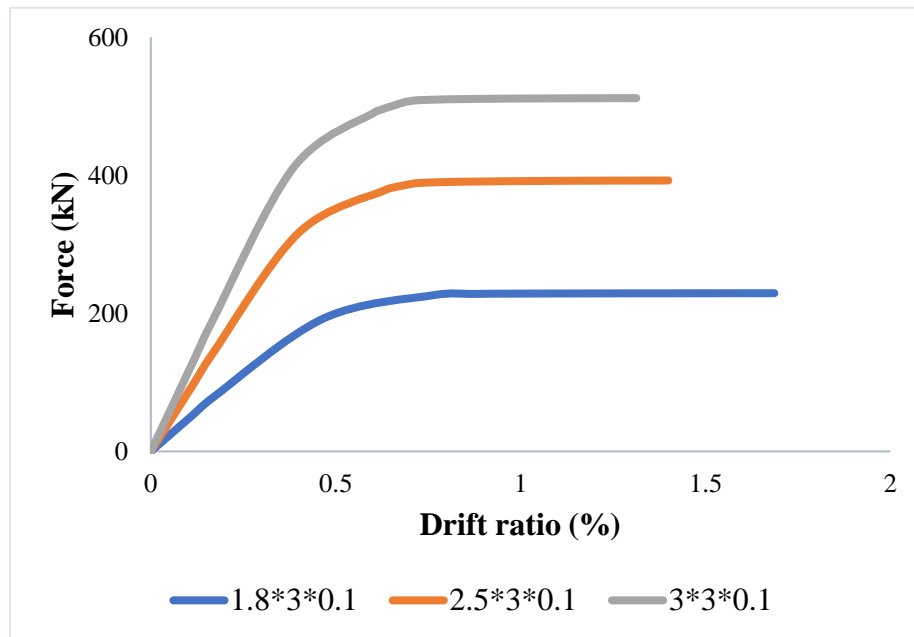


Fig.7.1 Load-drift ratio curve

- From Fig.7.1 we can understand that as the length of the wall increases, the load carrying capacity increases.
- When the length of the wall is increased from 1.8 m to 2.5 m (39 % increase in the length of wall) resulted in a 71% increase in load carrying capacity. And a further 28% increase in length of wall from 2.5m to 3.0m shows an increase of 56% increase in load carrying capacity of the infill wall. This also resulted in a linear dependence of the load carrying capacity with change in length of wall.
- This is because, as the length of the wall is increased keeping all other dimensions unchanged, the section modulus is increased. So, more force should

be given for creating an equal displacement in models with greater length of walls.

- From Fig.7.1 we can also understand that as the length of the wall increases, maximum top displacement attained is decreased.
- When the length of the wall is increased from 1.8 m to 2.5 m (39 % increase in the length of wall) resulted in a 17% decrease in top displacement. And a further 28% increase in length of wall from 2.5m to 3.0m shows an increase of 6% decrease in top displacement of the infill wall.
- This is because as the length of the wall is increased, the models become more and more stiffer and it require more force to show an equal displacement. This greater force in model with greater length resulted in the maximum strain in the diagonal and resulted in failure of the masonry wall.
- Here we can also see that in the initial increase in the length of the wall (1.8m to 2.5m), the top displacement is much sensitive to the increase in length, but in the later stage (2.5m to 3.0m), the dependence is much less.

7.1.1.2. Influence of height of wall

- To study the influence of the height of the infill wall, we have kept the other dimensions (thickness and length of the wall) as constant value as 0.1 and 1.8m respectively and only height of the wall is varied.

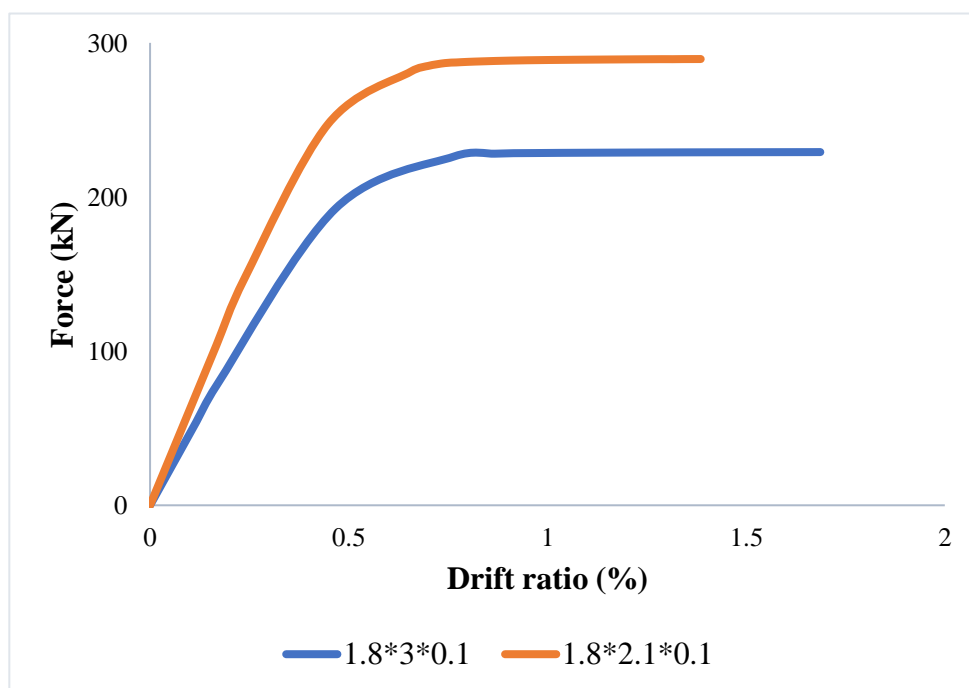


Fig.7.2 Load-drift ratio curve

- From Fig.7.2 we can understand that as the height of the wall increases, the load carrying capacity decreases.
- When the height of the wall is increased from 2.1 m to 3.0m (43% increase in the length of wall) resulted in a 21% decrease in load carrying capacity.
- From figure we can also understand that as the height of the wall increases, maximum top displacement attained is increased.
- When the height of the wall is increased from 1.8 m to 2.5 m (39 % increase in the height of wall) resulted in a 17% decrease in top displacement of infill wall.
- Mechanism of the modelled masonry wall is an exact replica of an inverted cantilever beam. We know that the deflection is proportional to the cube of the height of the wall. So, as the height of the wall is increased keeping all other dimensions unchanged, it can result in larger deflection for a comparable low applied force.

7.1.1.3. Influence of thickness of wall

- To study the influence of thickness of the infill wall, we have kept the other dimensions (height and length of the wall) as constant value as 3.0m and 1.8m respectively and only thickness of the wall was varied.
- From Fig.7.3 we can understand that as the thickness of the wall increases, the load carrying capacity increases.

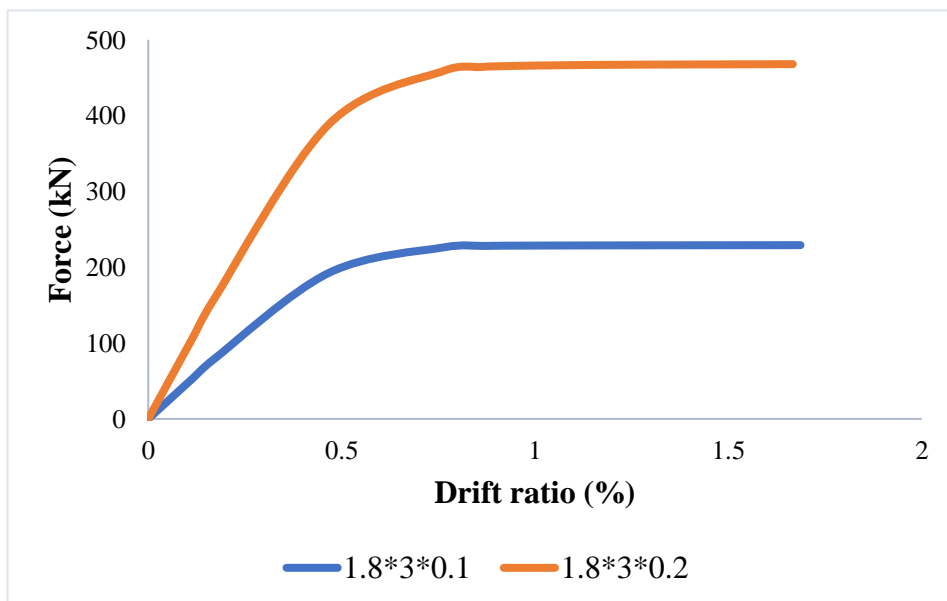


Fig.7.3 Load-drift ratio curve

- When the thickness of the wall is increased from 0.1 m to 0.2m (doubled), load carrying capacity was also doubled.
- This is because, as the thickness of the wall is increased keeping all other dimensions unchanged, the section modulus is increased. So, more force should be given for creating an equal displacement in models with more thickness of walls similar to that case of the length of wall.
- From Fig.7.3 we can also understand that change in thickness of the wall does not result in any change in the maximum top displacement obtained.

Fig.7.4 shows the comparison of the influence of length, height and thickness of infill wall based on load carrying capacity

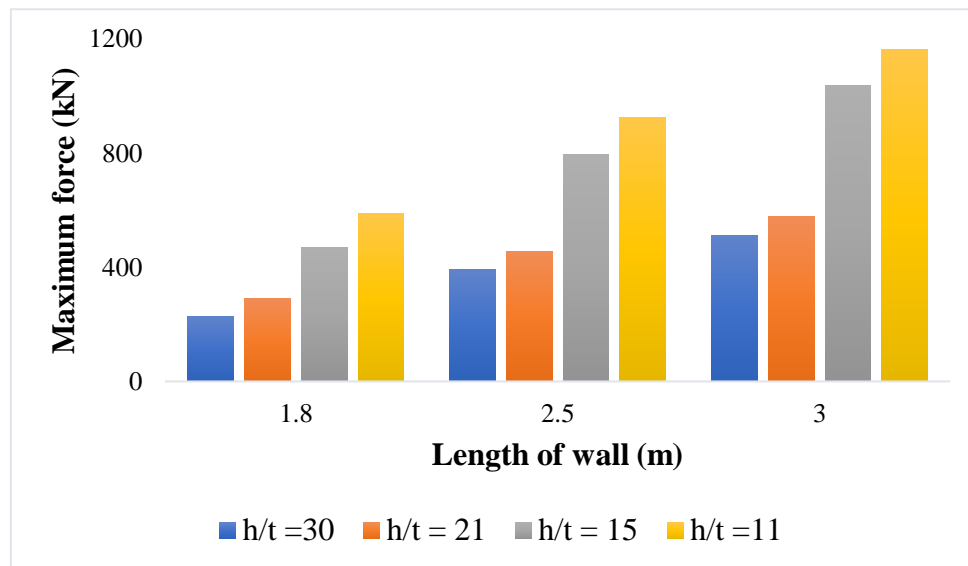


Fig.7.4 Variation of load with respect to changes in wall dimensions

From the above figure it is clear that as the length of the wall is increased, the load carrying capacity is improved. Also, we could see that as the height to thickness ratio (h/t) is reduced the load carrying capacity is improved.

7.1.2. Lateral Stiffness

- We know the initial lateral stiffness of the wall will be greater compared to the later stages of loading because in later stages of loading, some masonry units may be experiencing a plastic strain and thereby the strength of the material is lost.
- Fig.7.5 shows the variation of lateral stiffness corresponding to change in length of wall.

- As the length of wall is increased from 1.8m to 2.5m (39 % increase) resulted in an 82% increase in initial lateral stiffness. And with further increase in length from 2.5 to 3m (20% increase) resulted in 62% increase in initial lateral stiffness.
- The reason to the increase in initial lateral stiffness regarding to the change in length of wall is due to the increased section modulus.

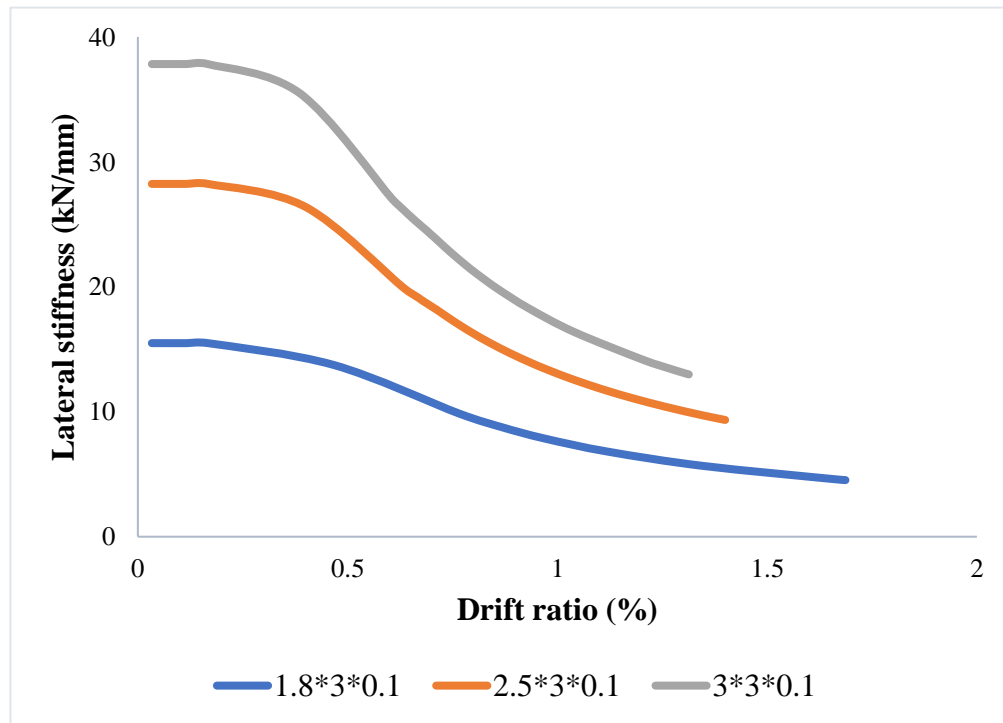


Fig.7.5 Lateral stiffness-drift ratio curve

- Fig.7.6 shows the variation of maximum initial lateral stiffness with the length, height and thickness of the wall.

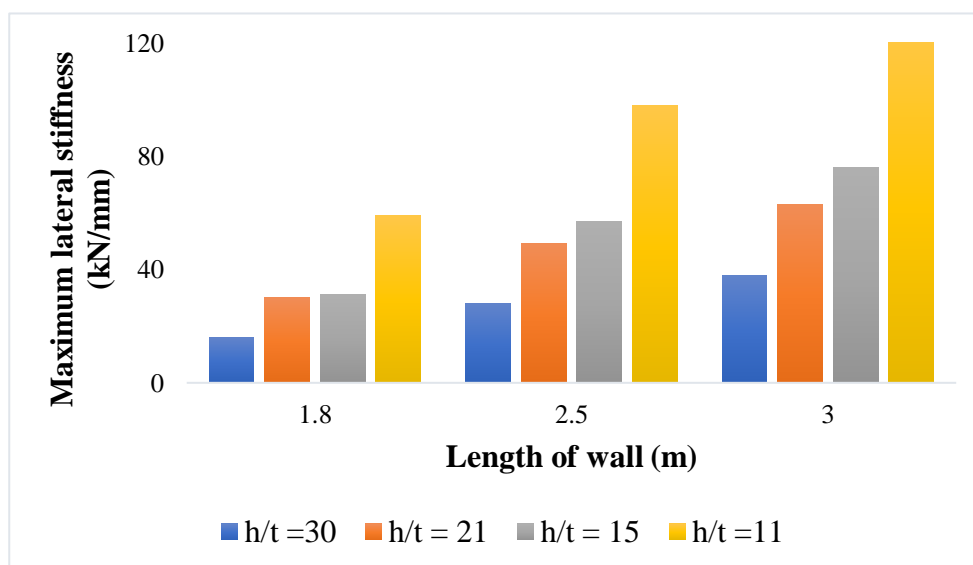


Fig.7.6 Variation of lateral stiffness with respect to changes in wall dimensions

- From Fig.7.6 it is clear that as the length of wall was increased the initial lateral stiffness in increased considerably and as the h/t ratio is reduced, the lateral stiffness is improved.

7.1.3. Energy dissipation

- To study the energy dissipation capacity of the structure, we had inputted the cyclic load and we measure the load versus displacement diagram as hysteresis loop as shown in Fig.7.7

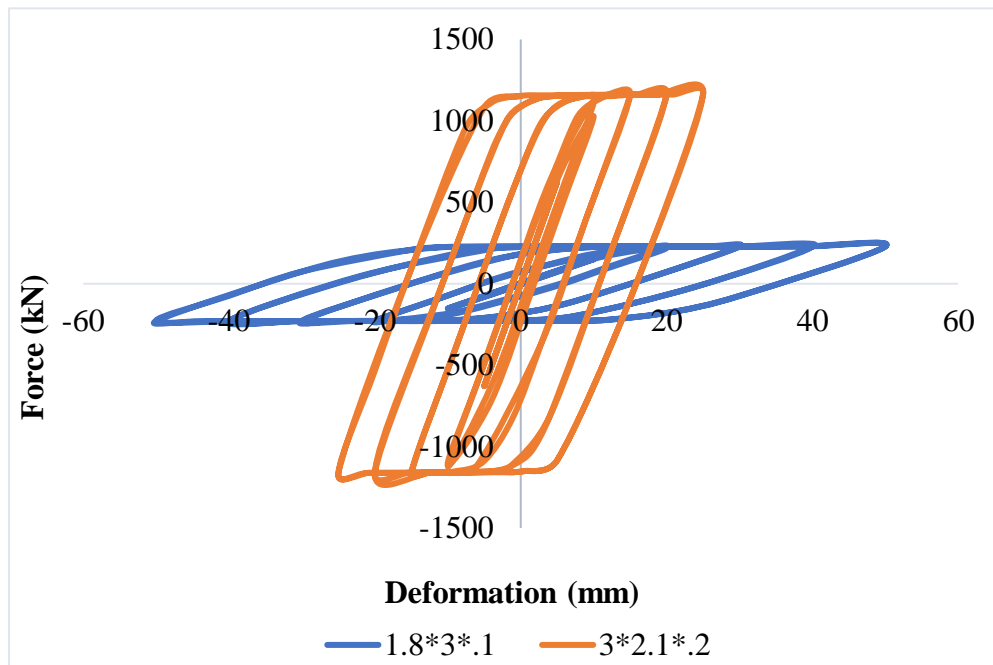


Fig.7.7 Hysteresis loop

- From the hysteresis loop we could only get a qualitative comparison and we could know that sample 3*2.1*.2 shows higher energy dissipation capacity than the 1.8*3*.1 sample.
- From the above graph we could also understand that the 3*2.1*.2 sample has larger stiffness compared to that of 1.8*3*.1 sample since the slope hysteresis loop of the 3*2.1*.2 sample is steeper than that of 1.8*3*.1.

- To get a quantitative value we had plotted cumulative energy dissipated graph as shown in Fig.7.8

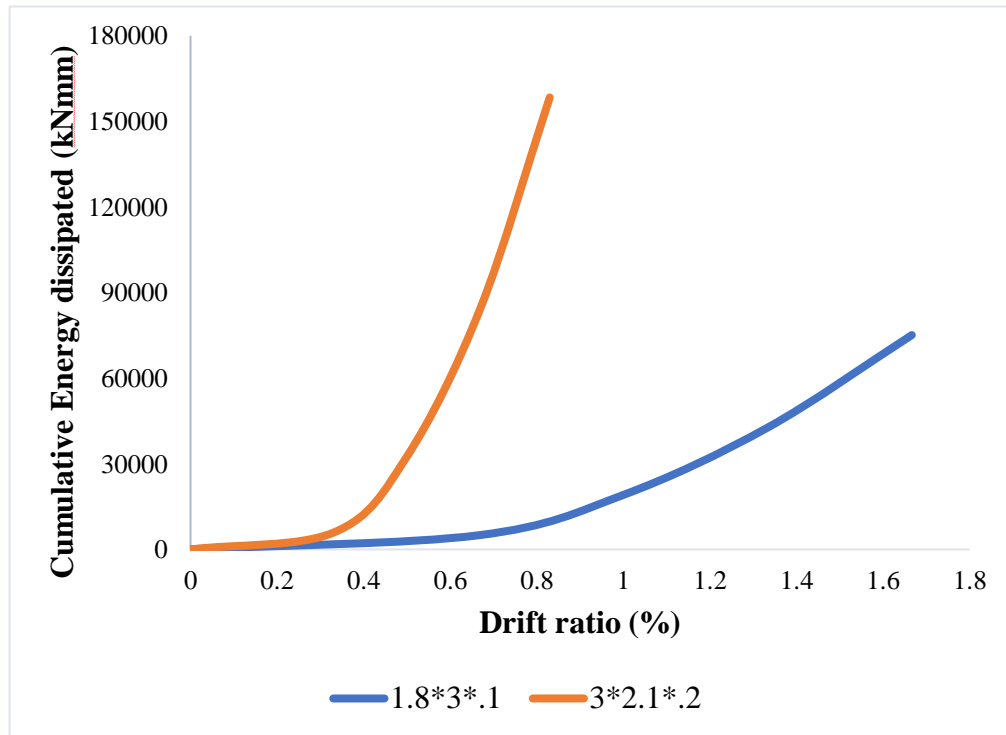


Fig.7.8 Cumulative energy dissipation curve

- From the above graph we could clearly interpret that the 3*3*.2 sample shows greater energy dissipation capacity than that of 1.8*3*.1 sample
- This was because as the length of the wall was increased, the section modulus had improved and thereby the strength was improved. Also, as the deflection is directly related to height as height is reduced the sample become more and more stiff and further resisting higher load.

7.2. PERFORMANCE EVALUATION OF MASONRY INFILL WALLS WITH CONFINING FRAME

7.2.1. Failure mechanism

Since we were following the macro modelling, we will not be able to simulate all the failure mechanism. As we had considered the brick masonry as a single unit, we cannot replicate the horizontal slipping along the mortar joints. But we were able to show the diagonal compression and crushing of corners as shown in Fig.7.9

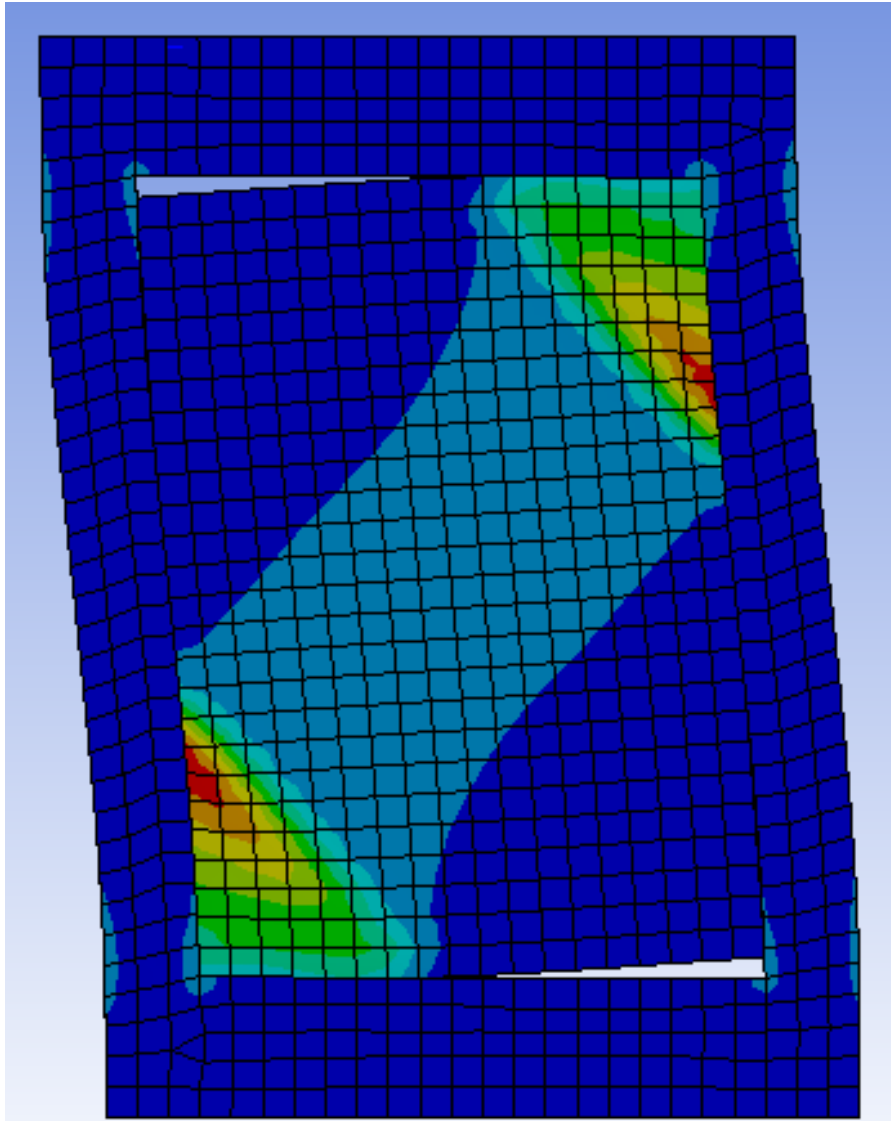


Fig.7.9 Failure mechanism

7.2.2. Load carrying capacity

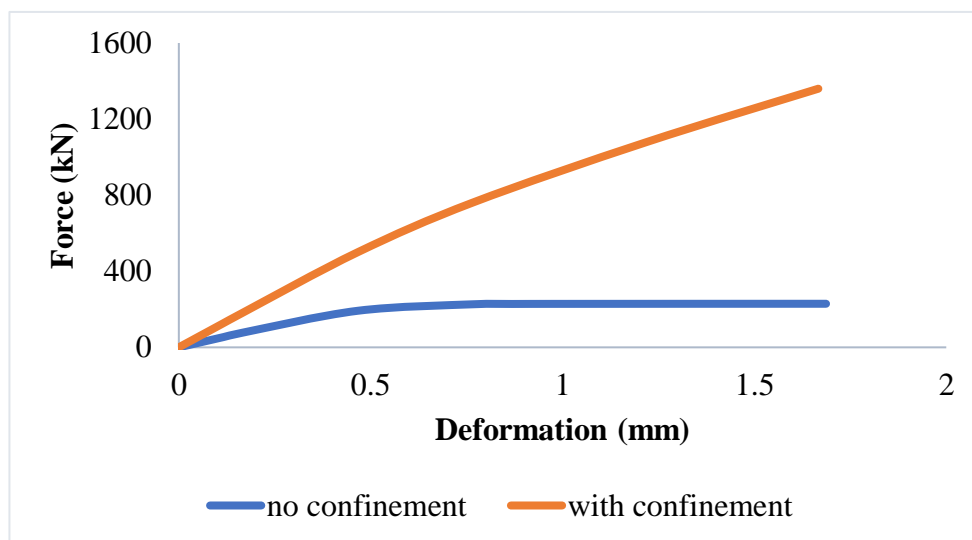


Fig.7.10 Load-drift ratio curve

- From Fig.7.10 it is clear that masonry wall with confining frame outperformed unconfined models.
- With the confining frame the lateral load carrying capacity is increased by 6 times.
- The reason is that with the addition of the confining frame the applied load is counteracted by the combination of masonry wall and the frame. The frame is much stiffer compared to the masonry wall and takes the applied load and that is why the lateral load carrying capacity is improved for the samples with confining frame.

7.2.3. Lateral Stiffness

- Fig.7.11 shows the variation of lateral stiffness corresponding to the drift ratio.
- It is clear from the figure that by the addition of confining frame the lateral stiffness is improved by 2.5 times
- The reason behind this is that with the addition of confining frame which is much stronger in taking the loads compared to that of the masonry wall. So, the applied load to the confined masonry wall will be taken by the combined action of frame as well as the masonry wall which results in higher stiffness

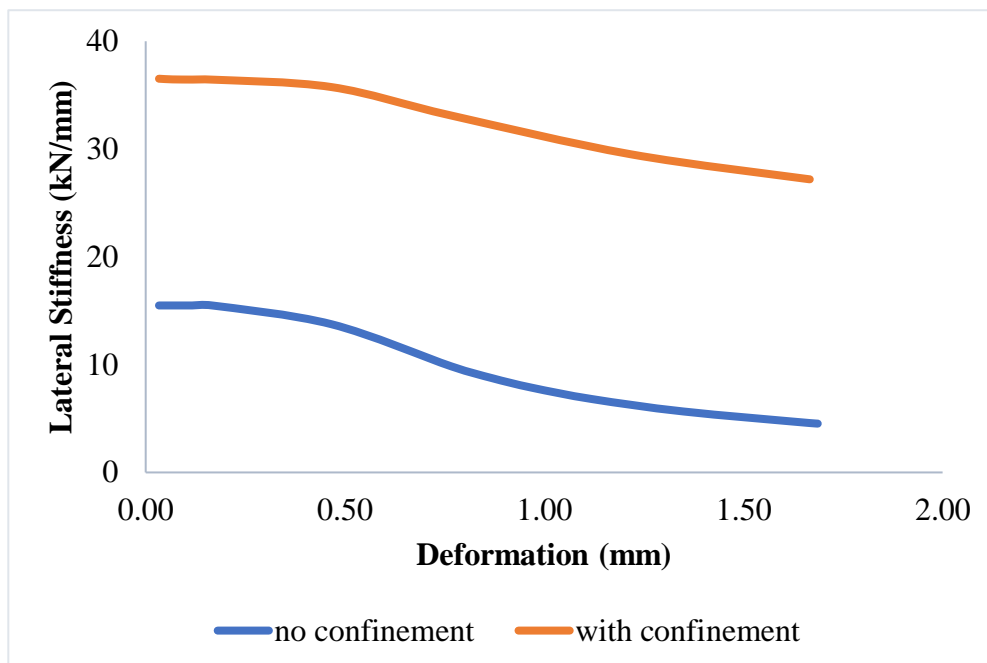


Fig.7.11 Lateral stiffness-drift ratio curve

7.2.4. Energy dissipation

- Fig.7.12 shows the hysteresis curve of the unconfined masonry as well as the confined masonry wall
- Hysteresis loop only gives a qualitative approach and from the figure we could interpret that the energy dissipation of both these models is almost similar. To quantify the energy dissipation, we need to take a look at the cumulative energy dissipation curve drawn in Fig.7.13.

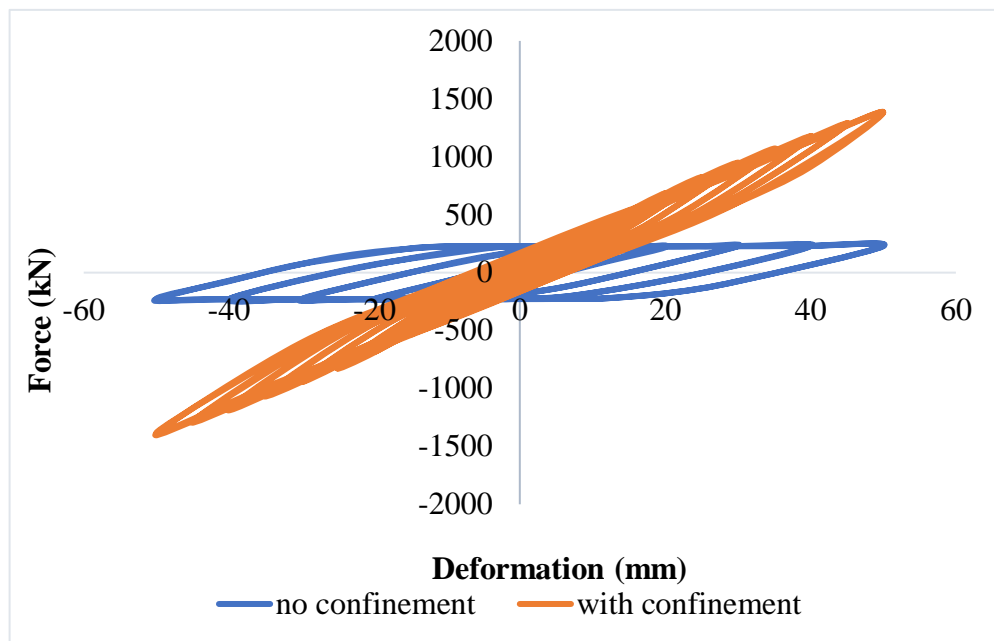


Fig.7.12 Hysteresis loop

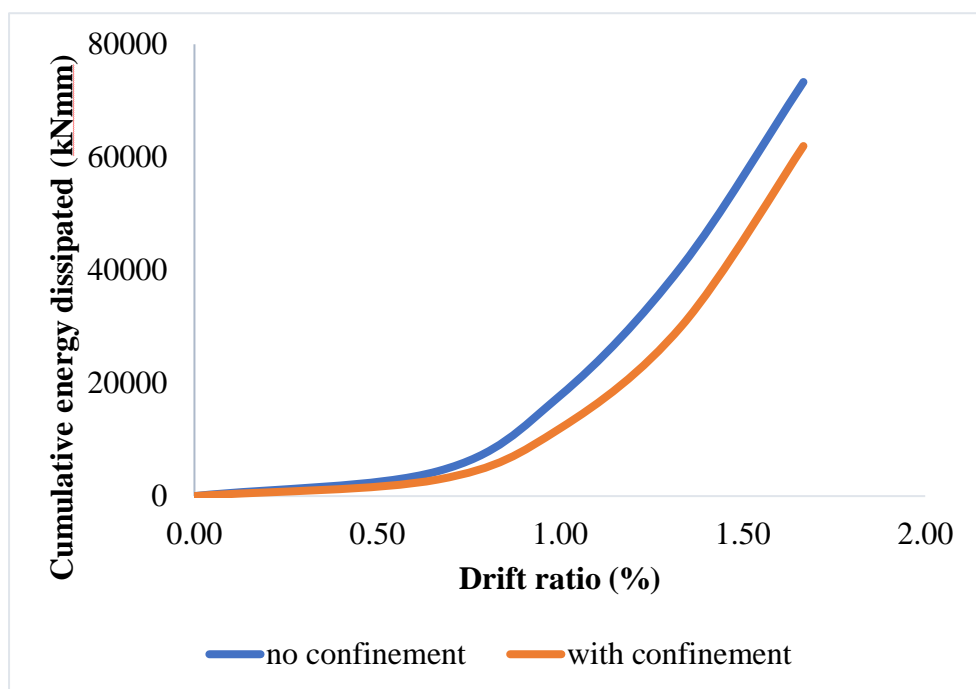


Fig.7.13 Cumulative energy dissipation curve

- From Fig.7.13 we can see that model with on confinement shows improved energy dissipation capacity that that of confined one. About 15 % reduction in energy dissipation capacity is observed in the confined model to that of unconfined model
- The reduction in energy dissipation for the confined models can be due to many reasons. One of the main reasons is that in modelling we had modelled the contact interface as sliding or frictional surface but in actual case the joint between concrete frame and masonry act as fixed ones and only after a particular load the bond is broken and act as a sliding surface. Other reason is that by providing the frame, the masonry had not reached ultimate strain in the given loads which resulted in lesser dissipation capacity.

7.3. PERFORMANCE EVALUATION OF MASONRY INFILL WALLS WITH LINTEL BEAMS

7.3.1. Load carrying capacity

- Fig.7.14 shows the comparison of load carrying capacity of sample with no lintel beam and other with lintel beam.
- It is clear from the figure that as we could understand that as we provide lintel beam the load carrying capacity is increased 3 times.

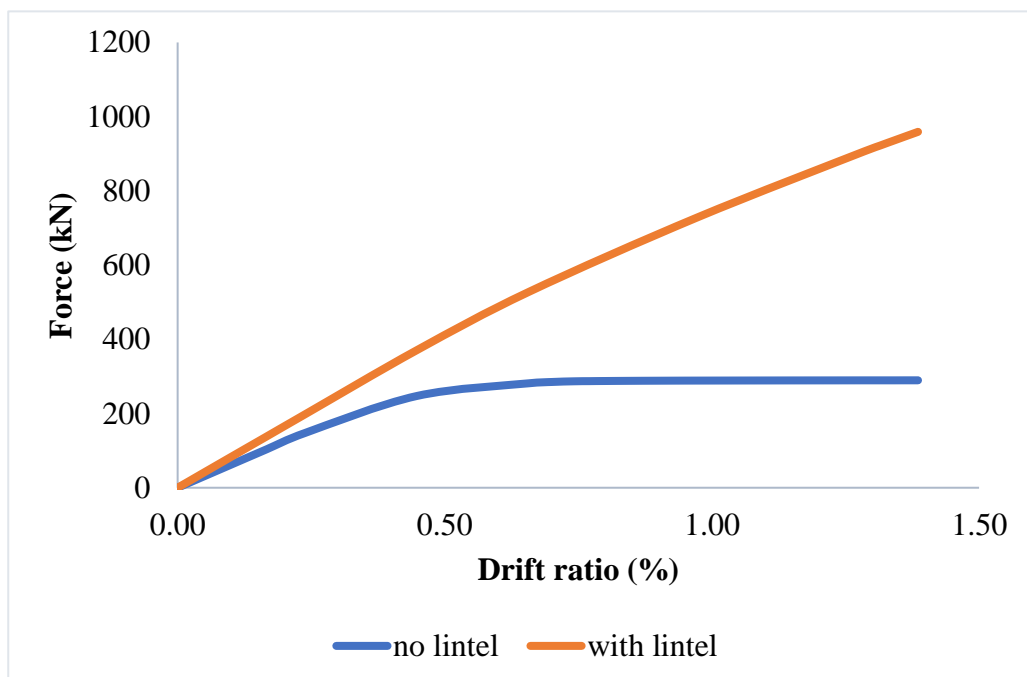


Fig.7.14 Load drift ratio curve

- The reason behind this was that, by the introduction of lintel beams the masonry wall below the lintel beams is converted to a confined wall and that was why the lateral load carrying capacity is improved.

7.3.2. Lateral Stiffness

- Fig.7.15 shows the variation in lateral stiffness corresponding to different drift ratios.
- From the graph it is clear that as we incorporate lintel beam into the samples, the initial lateral stiffness is increases about 33%.
- The reason behind the increase in the lateral stiffness due to the addition of lintel beams was due to the confining effect provided by the lintel beams to the masonry walls

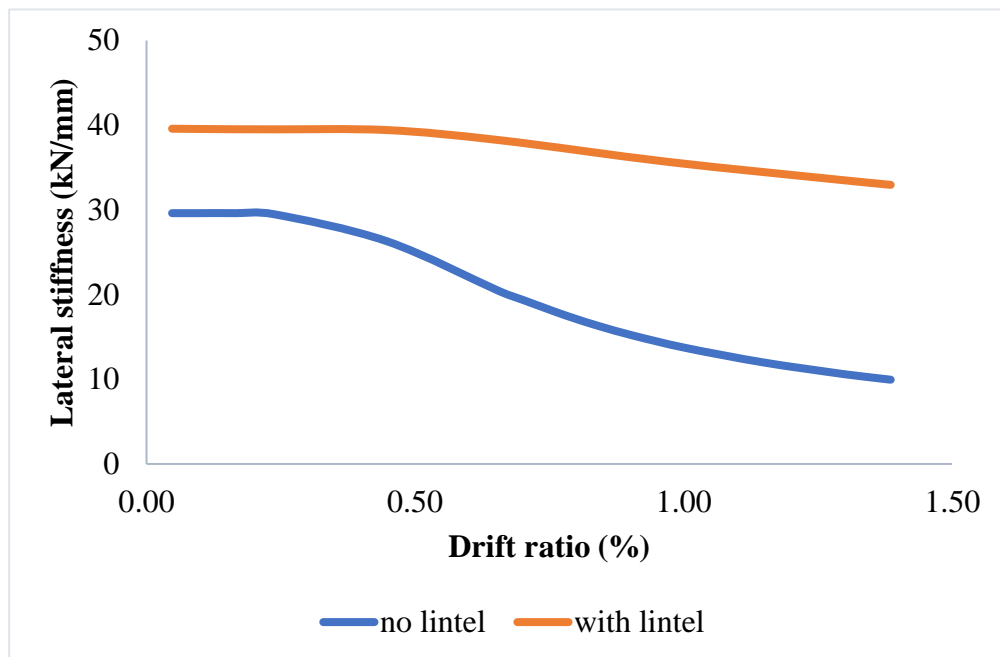


Fig.7.15 Variation of lateral stiffness

8.3.3. Energy dissipation

- Fig.8.16 shows the comparison of hysteresis loop of sample without lintel beam and sample with lintel beam.
- From the hysteresis loop we could qualitatively estimate that the energy dissipation capacity of the sample with lintel beam is lesser that that of unconfined sample. But to quantify the energy dissipation we had plotted the cumulative energy dissipation curve as shown in Fig.7.17

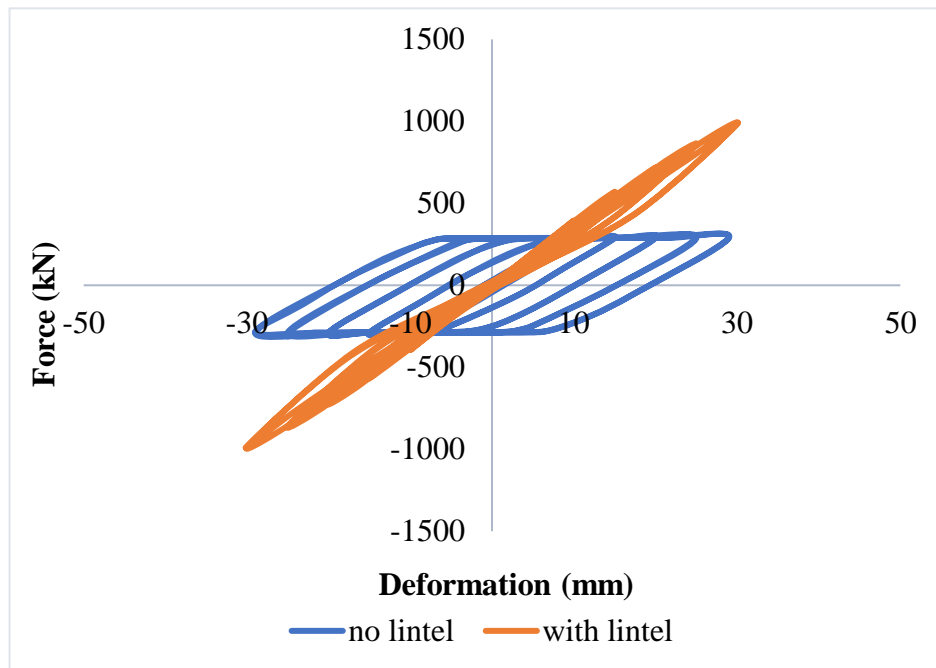


Fig.7.16 Hysteresis loop

- From Fig.7.17 we could understand that the energy dissipation capacity of sample with lintel beam is reduced by 65%

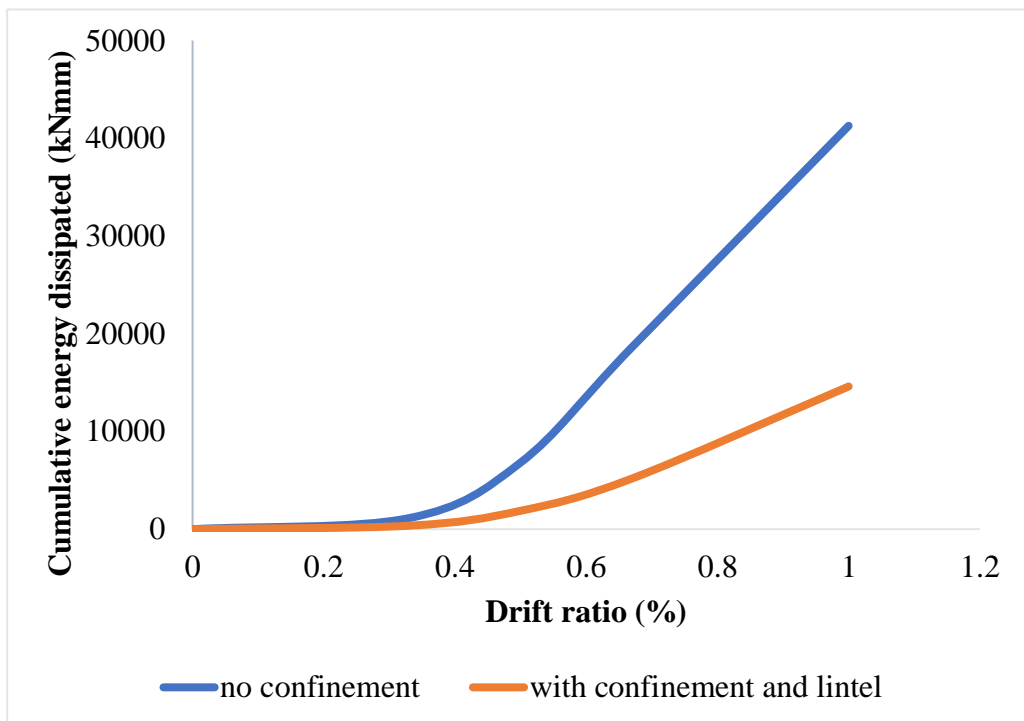


Fig.7.17 Cumulative energy dissipation curve

- The reduction in energy dissipation for the models with lintel beams can be due to many reasons. One of the main reasons is that in modelling we had modelled the contact interface as sliding or frictional surface but in actual case the joint

between concrete frame and masonry act as fixed ones and only after a particular load the bond is broken and act as a sliding surface. Other reason is that by providing the frame, the masonry had not reached ultimate strain in the given loads which resulted in lesser dissipation capacity.

7.4. PERFORMANCE EVALUATION OF MASONRY INFILL WALLS WITH OPENINGS

7.4.1. Effect of size of openings

7.4.1.1 Load carrying capacity

- Fig.7.18 the variation of load carrying capacity with respect to the different opening size.

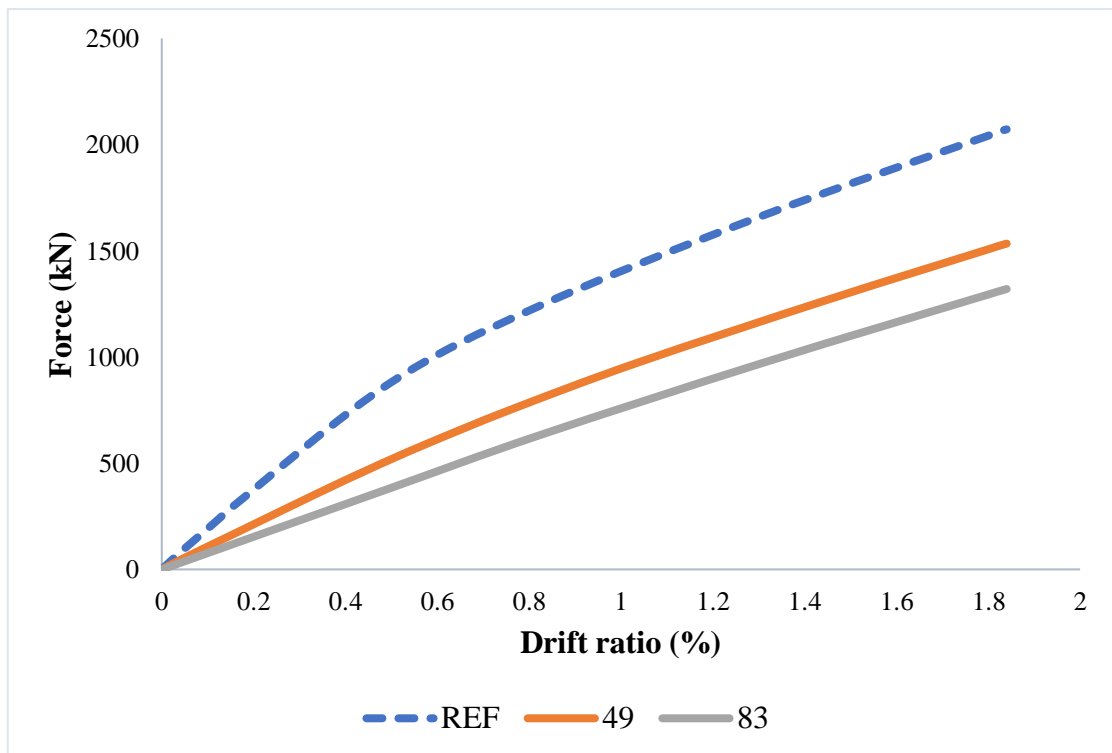


Fig.7.18 Load-drift ratio curve

- From the graph it is clear that as the opening size is increased the lateral load carrying capacity of the structure is reduced considerably
- As the opening size is increased from 0 to 49 %, the lateral load carrying capacity is reduced by 26% and further increase of opening size from 49 to 83% resulted in only 10% reduction in lateral load carrying capacity.

- Reduction in load carrying capacity is due to the loss of material from the masonry wall. This reduces the stiffness and thereby the load carrying capacity is reduced.

7.4.1.2. Lateral Stiffness

- Fig.7.19 shows the variation of lateral stiffness of the samples by changing the area of openings.

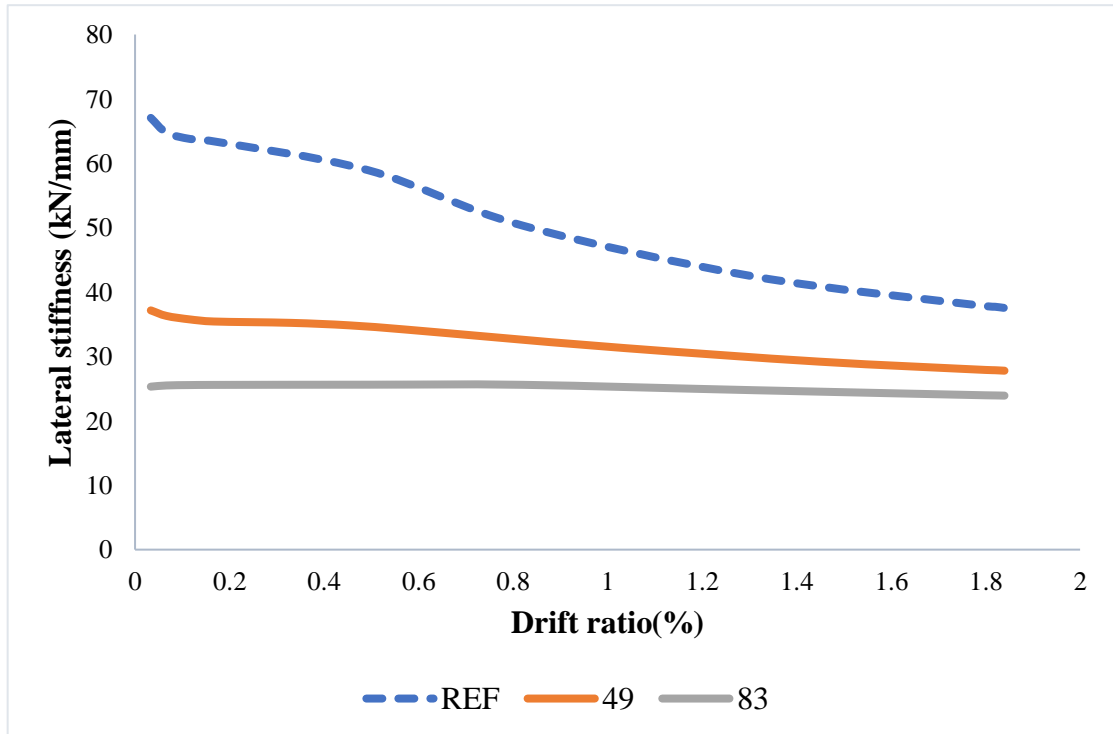


Fig.7.19 Lateral stiffness-drift ratio curve

- As shown in graph we can understand that as the area of opening is increased from 0 to 49% the initial lateral stiffness is reduced by 45% and a further increase in area of opening from 49 to 83 % resulted in only 17% reduction.
- The reason behind the reduction in lateral stiffness is due to the loss of material in increasing the area of openings. As the load is increased there is no sufficient material to resist the loading.

7.4.1.3. Energy dissipation

- Fig.7.20 shows the variation of cumulative energy dissipation of models with different area of openings
- From the graph it is clear that as the area of opening is increased the energy dissipation capacity of the structure is reduced. As the area of opening is

increased from 0 to 49 % the energy dissipation is reduced by 66% and further increase in opening size from 49 to 83 % resulted in 22 % reduction in energy dissipation.

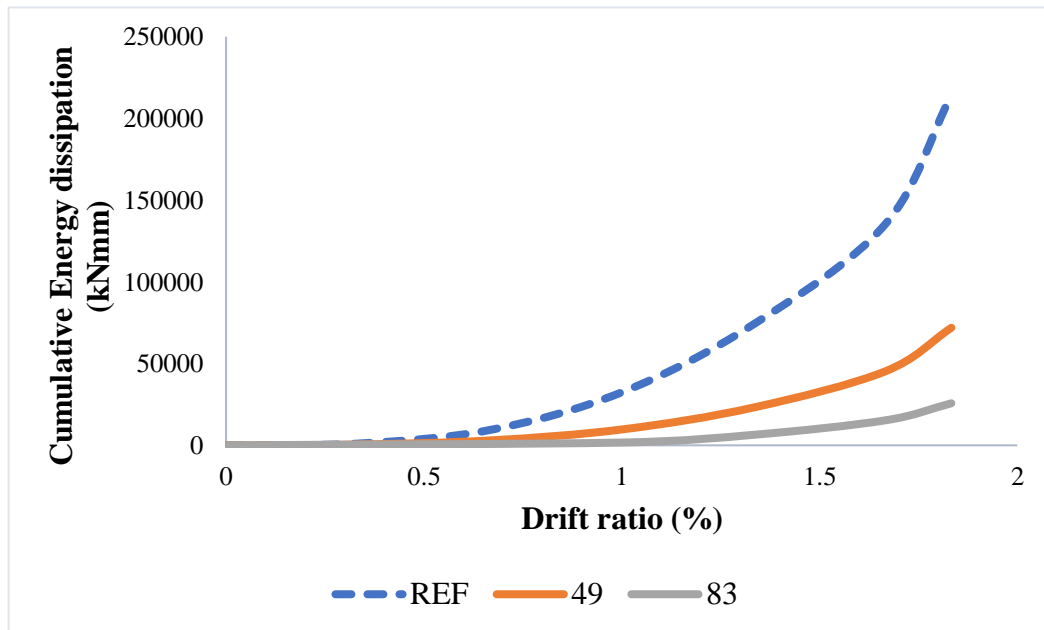


Fig.8.20 Cumulative energy dissipation

- This is because as the area of opening is increased the masonry material is reduced so there will be a loss of material which results in reduction in energy dissipation.

7.4.2. Effect of placement of openings

7.4.2.1. Load carrying capacity

- Fig.7.21 shows the plot between load carrying capacity and drift ratio for different placement of openings
- The size of the opening was kept constant and only the placement has been changed as shown in Fig.7.21
- From sample (a) to sample (c) the load carrying capacity had been reduced by 29% and from sample (c) to (b) the load carrying capacity had been reduced by only 6%
- The reason behind the lower load carrying capacity of sample (b) than that of sample (c) is that in sample (b) the openings were closer towards the diagonals.

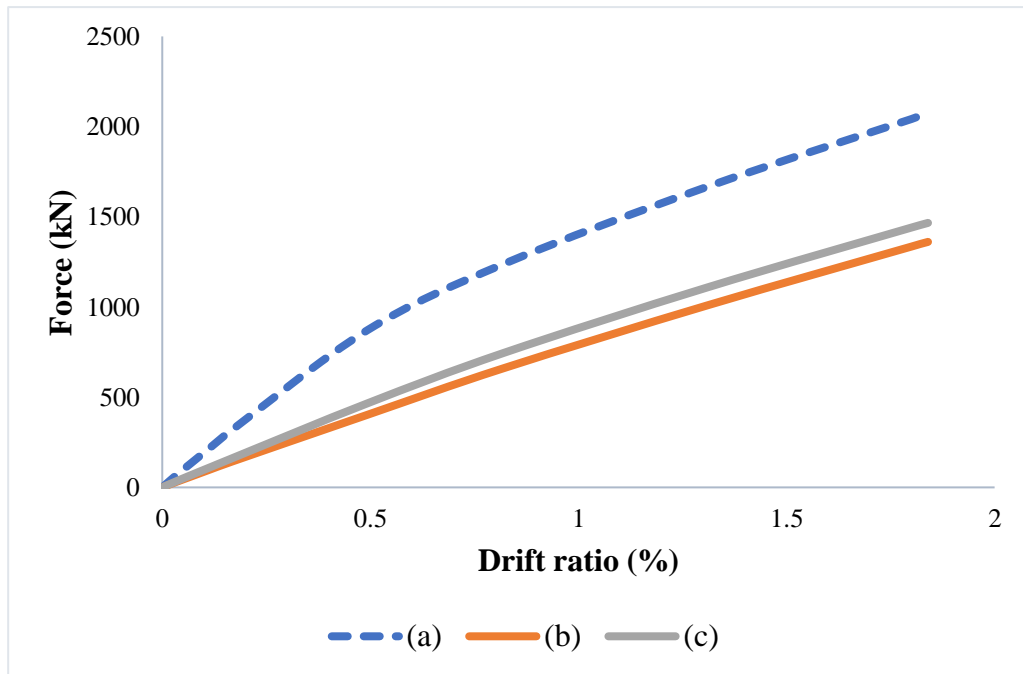


Fig.7.21 Force-drift ratio curve

7.4.2.2. Lateral Stiffness

- Fig.7.22 shows the variation of lateral stiffness with respect to the applied drift loads for different orientation of openings.

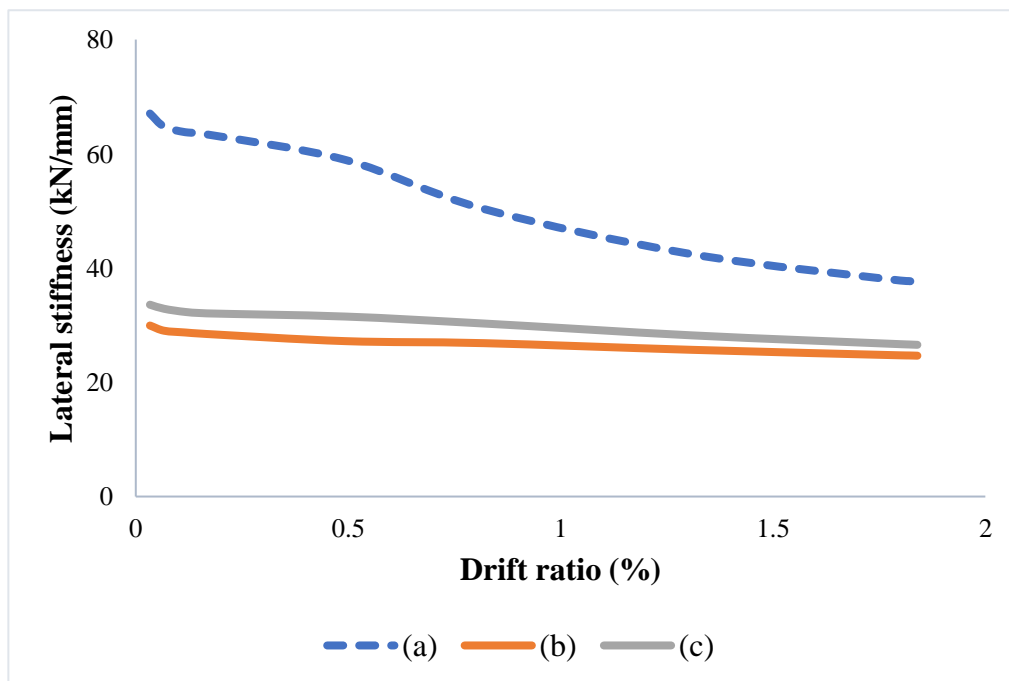


Fig.7.22 Lateral stiffness-drift ratio curve

- From the graph it is clear that as the orientation of the openings were changed the lateral stiffness was changed.

- From sample (a) to (c) the initial lateral stiffness is reduced about 50% and from sample (c) to (b) the lateral stiffness is reduced by about 5%.
- This is because in sample (b) the openings are oriented more towards the diagonal. So, the resistance offered to the applied load is less.
- Also, here we can understand that the change in orientation of the openings cause only small changes. This is because in our study we had only taken a single wall but for a high rise building the change will be significant enough.

7.4.2.3. Energy dissipation

- Fig.7.23 represent the cumulative energy dissipation of models with different orientation of openings.

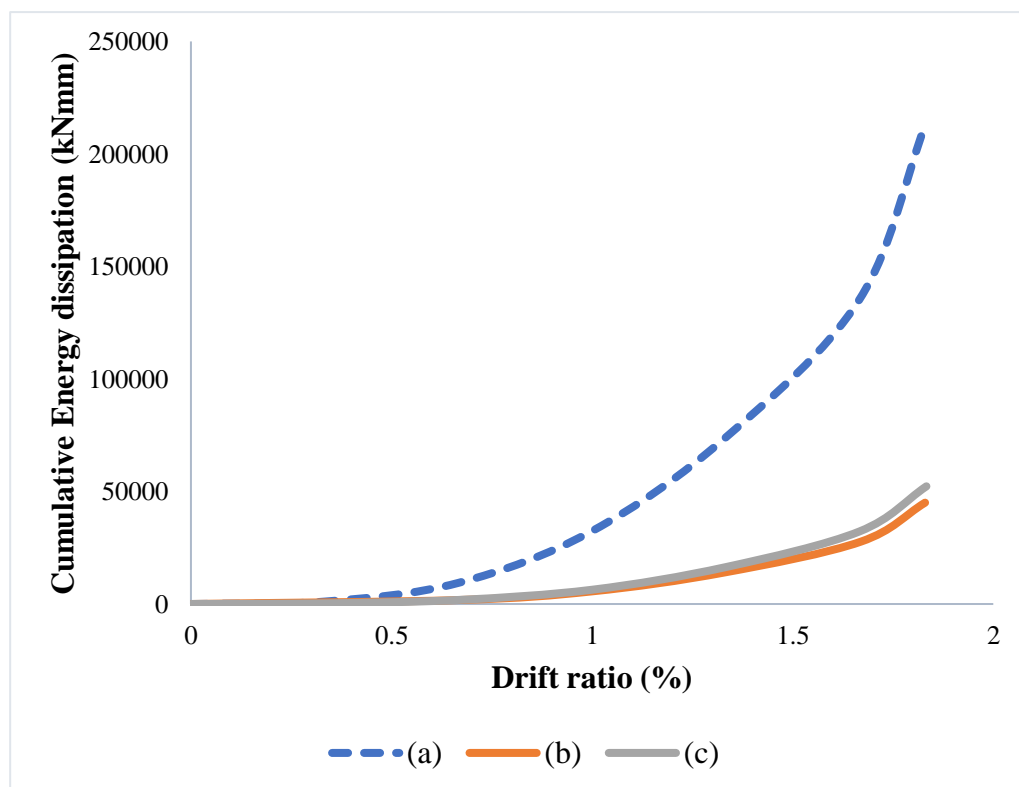


Fig.7.23 Cumulative energy dissipation

- Here also we can see that from sample (c) to (b) the cumulative energy dissipation is reduced only 3%. The reduction is caused because in sample (b) the openings are closer to the diagonal.
- The reduction in cumulative energy dissipation is very negligible because we had only considered a single wall but in an actual high rise building the change will be significant.

CHAPTER 8

CONCLUSION

8.1. GENERAL

Since there are many parameters that can affect the performance of the masonry wall numerical analysis is justified. Also, in our study we had used acro-modelling which only gives an approximate result rather than accurate results.

8.2. MAJOR FINDINGS

In the initial phase of study, we had done analysis on unconfined masonry wall and had found out that:

- Increase in length and thickness of the wall improves the load carrying capacity, lateral stiffness and energy dissipation capacity.
- Decrease in the height of wall resulted in the improvement in load carrying capacity, lateral stiffness and energy dissipation.

Next, we had analysed masonry wall with confining frame and had found that:

- Presence of confining frame resulted in improving the load carrying capacity and lateral stiffness.
- But the presence of confining frame also had resulted in lesser energy dissipation capacity for the given drift ratio.

Next, we had studied the influence of lintel beams and had found that:

- Presence of lintel beams had improved the load carrying capacity and lateral stiffness.
- We had also noted that the presence of lintel beams had resulted in a reduction in energy dissipation capacity for a given drift ratio

Finally, we had introduced the combination of openings and had studied the influence of lateral loads on it and we had found out that:

- As the area of opening is increased, the lateral load carrying capacity, lateral stiffness and energy dissipation capacity has been decreased.

- Also, we had studied the influence of orientation of openings and found out that, as we place the openings closer towards the diagonals, the load carrying capacity, lateral stiffness and energy dissipation capacity had been reduced.

8.3. FUTURE SCOPE

The proposed study has its own limitations which should be taken into consideration in future works. Future studies should focus on the following:

- Micro-modelling could be done so as to get a clear representation of the actual behaviour
- Modelling of a whole building would give more clear insight of the scenario.
- Out of plane behaviour could be incorporated

REFERENCES

1. Bikce, M., Emsen, E., Erdem, M. M., and Bayrak, O. F. (2021). “An investigation on behavior of RC frames with non-interacting infill wall.” *Engineering Structures*, Elsevier Ltd, 245(June), 112920.
2. Baniahmedi, M., Vafaei, M., and Alih, S. C. (2022). “Cyclic response of reinforced concrete frames partially infilled with relatively weak masonry wall.” *Journal of Building Engineering*, Elsevier Ltd, 46(November 2021), 103722.
3. Borsaikia, A. C., Dutta, A., and Deb, S. K. (2021). “Evaluation of participation of masonry infill walls in the linear and nonlinear behaviour of RC buildings with open ground storey.” *Journal of Building Engineering*, Elsevier Ltd, 44(June), 103263.
4. Campbell, J., and Durán, M. (2017). “Numerical model for nonlinear analysis of masonry walls.” *Revista de la Construcción*, 16(2), 189–201.
5. Deb, T., Yuen, T. Y. P., Lee, D., Halder, R., and You, Y. C. (2021). “Bi-directional collapse fragility assessment by DFEM of unreinforced masonry buildings with openings and different confinement configurations.” *Earthquake Engineering and Structural Dynamics*, 50(15), 4097–4120.
6. Dhir, P.K., Tubaldi, E., Ahmadi, H., and Gough, J. (2021). “Numerical modelling of reinforced concrete frames with masonry infills and rubber joints.” *Engineering Structures*, Elsevier Ltd, 246(January), 112833.
7. Dilmac, H., Ulutas, H., Tekeli, H., and Demir, F. (2018). “The investigation of seismic performance of existing RC buildings with and without infill walls.” (November).
8. Feba, S. T., and Kuriakose, B. (2016). “Nonlinear Finite Element Analysis of Unreinforced Masonry Walls.” *Applied Mechanics and Materials*, 857(January), 142–147.
9. Furtado, A., Rodrigues, H., and Arede, A. (2021). “Effect of the infill panels in the floor response spectra of an 8-storey RC building.” 34(September), 2476–2498.
10. Guevara, L. T., and García, L. E. (2005). “The captive- and short-column effects.” *Earthquake Spectra*, 21(1), 141–160.

11. Jalaeefar, A., and Zargar, A. (2020). "Effect of infill walls on behaviour of reinforced concrete special moment frames under seismic sequences." *Structures*, Elsevier, 28(May), 766–773.
12. Kaushik, H. B., Rai, D. C., and Jain, S. K. (2007). "Stress-Strain Characteristics of Clay Brick Masonry under Uniaxial Compression." *Journal of Materials in Civil Engineering*, 19(9), 728–739.
13. Keyvani, J., and Farzadi, M. (2011). "Impact of brick infill walls on the seismic behaviour of reinforced concrete frames using finite element method." *Asian Journal of Civil engineering (Building and housing)*, 12(6), 789-802.
14. Khan, N. A., Nuti, C., and Briseghella, B. (2019). "Influence of Brick Masonry Infill Walls on Seismic Response of RC Structures." (August 2020).
15. Koutromanos, I., Stavridis, A., Shing, P. B., and Willam, K. (2011). "Numerical modeling of masonry-infilled RC frames subjected to seismic loads." *Computers and Structures*, Elsevier Ltd, 89(11–12), 1026–1037.
16. Kumbasaroglu, A., Yalciner, H., and Firdes Aydin, Y. (2017). "The effect of infill wall frames on seismic performance levels of RC buildings." International Conference on Structural Engineering Dynamics, (January).
17. Marinković, M., and Butenweg, C. (2019). "Innovative decoupling system for the seismic protection of masonry infill walls in reinforced concrete frames." *Engineering Structures*, Elsevier, 197(July), 109435.
18. Mehrabi, A. B., Schuller, M. P., and Noland, J. L. (1996). "Experimental evaluation of masonry-infilled frames." 89, 228–237.
19. Motwani, P., Rajendhiran, and Santhi, A. S. (2015). "Simulation of brick infill and effect of openings on RC frames using ANSYS." *Indian Journal of Science and Technology*, 8(January), 29–35.
20. Naciri, K., Aalil, I., Chaaba, A., and Al-Mukhtar, M. (2022). "Numerical analysis of the brick shape and bond pattern effects on the masonry cyclic behavior: a new brick shape to improve the masonry seismic performance." *Asian Journal of Civil Engineering*, Springer International Publishing, 23(1), 67–86.
21. Nasiri, E., and Liu, Y. (2017). "Development of a detailed 3D FE model for analysis of the in-plane behaviour of masonry infilled concrete frames." *Engineering Structures*, Elsevier Ltd, 143, 603–616.

22. Okasha, M. A. T. A., Abdel Razek, M., and El-Esnawi, H. (2020). “Strengthening of existing RC buildings by using autoclaved aerated concrete infill wall.” *HBRC Journal*, Taylor & Francis, 16(1), 143–155.
23. Pachappoyil, N. S., and Agarwal, P. (2021). “Performance evaluation of the energy dissipating hysteretic infill wall frame considering opening under in-plane and out-of-plane loading.” *Engineering Structures*, Elsevier Ltd, 249(September), 113329.
24. Pallar, F. J., Davia, A., Hassan, W. M., and Pallar, L. (2021). “Experimental and analytical assessment of the influence of masonry façade infills on seismic behavior of RC frame buildings.” 235(September 2020).
25. Park, C. Y., Kim, H. K., Eom, C. D., Kim, G. C., and Lee, J. J. (2014). “Effect of lintel on horizontal load-carrying capacity in post-beam structure.” *Journal of Wood Science*, 60(1), 30–38.
26. Pudjisuryadi, P., Prayogo, V. S., Oetomo, S. I., and Lumantarna, B. (2021). “Seismic Performance of a Three-Story Reinforced Concrete Building with Masonry Infill Walls and Friction Base Support.” *Civil Engineering Dimension*, 23(1), 35–43.
27. Rahem, A., Djarir, Y., Nouredine, L., and Tayeb, B. (2021). “Effect of Masonry Infill Walls with Openings on Nonlinear Response of Steel Frames.” 7(02), 278–291.
28. Rodrigues, H. (2021). “Experimental and numerical assessment of confined infill walls with openings and textile-reinforced mortar.” 151(September).
29. Shendkar, M. R., Kontoni, D. P. N., Mandal, S., Maiti, P. R., and Gautam, D. (2021). “Effect of lintel beam on seismic response of reinforced concrete buildings with semi-interlocked and unreinforced brick masonry infills.” *Infrastructures*, 6(1), 1–18.
30. Stavroulaki, M. E., and Liarakos, V. B. (2012). “Dynamic analysis of a masonry wall with reinforced concrete lintels or tie-beams.” *Engineering Structures*, Elsevier Ltd, 44, 23–33.
31. Tamboli, H., and Karadi, U. (2012). “Seismic Analysis of RC Frame Structure with and without Masonry Infill Walls.” *Indian Journal of Natural Sciences*, 3(14), 1137–1148.

32. Uva, G., Porco, F., and Fiore, A. (2012). “Appraisal of masonry infill walls effect in the seismic response of RC framed buildings: A case study.” *Engineering Structures*, Elsevier Ltd, 34, 514–526.

LIST OF PUBLICATIONS

International Conference

1. Isac T. K., Bushra M. A. (2022). “Performance evaluation of unconfined masonry infill walls.” *Proceedings of the 2nd International Conference on Recent Trends in Engineering Technology Management 2022*, 70-71